

AD-A086 809

EPSILON LABS INC BEDFORD MA
SATELLITE DENSITY GAUGE INSTRUMENTATION PROGRAM. (U)
JAN 80 C A ACCARDO, J DULCHINOS

F/6 9/1

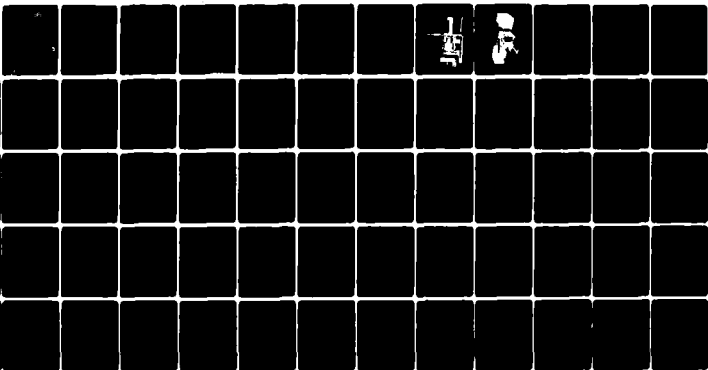
F19628-77-C-0062

AFGL-TR-80-0036

ML

UNCLASSIFIED

Fig 1
of 6
Reels



END
DATE
FILMED
8-80
DTIC

ADA 086809

LEVEL

12

AFGL-TR-80-0036

Instrumentation

SATELLITE DENSITY GAUGE PROGRAM

Carl A. Accardo
John Dulchinos

Epsilon Laboratories, Inc.
4 Preston Court
Bedford, MA 01730

January 1980

Final Report for period January 11, 1977 to December 30, 1978

Approved for public release; distribution unlimited.

Air Force Geophysics Laboratory
Air Force Systems Command
United States Air Force
Hanscom AFB, MA 01731

OPTIC
ECTE
JUL 17 1980
D

DDC FILE COPY

80 7 16 01

Qualified requestors may obtain additional copies from the Defense Documentation Center. All others should apply to the National Technical Information Service

UNCLASSIFIED

SECURITY CLASSIFICATION OF THIS PAGE (When Data Entered)

19 REPORT DOCUMENTATION PAGE		READ INSTRUCTIONS BEFORE COMPLETING FORM	
1. REPORT NUMBER 18 AFGL TR-80-0036	2. GOVT ACCESSION NO. AD-A086809	3. RECIPIENT'S CATALOG NUMBER	
4. TITLE (and Subtitle) 6 SATELLITE DENSITY GAUGE INSTRUMENTATION PROGRAM		9. TYPE OF REPORT & PERIOD COVERED Final rept. 1 Jan 1977 to Dec 1978	
7. AUTHOR(s) 10 Carl A. Accardo John Dulchinos		8. CONTRACT OR GRANT NUMBER(s) 15 F19628-77-C-0062 F19628-74-C-0156 30	
9. PERFORMING ORGANIZATION NAME AND ADDRESS Epsilon Laboratories, Inc./ 4 Preston Court Bedford, MA 01730		10. PROGRAM ELEMENT, PROJECT, TASK AREA & WORK UNIT NUMBERS 62101F 669002 AP 16 17 02	
11. CONTROLLING OFFICE NAME AND ADDRESS Air Force Geophysics Laboratory Hanscom Air Force Base, Massachusetts 01731 Contract Monitor: Joseph McIsaac/LKB		12. REPORT DATE 11 Jan 1980	
14. MONITORING AGENCY NAME & ADDRESS (if different from Controlling Office)		13. NUMBER OF PAGES 68	
12 72		15. SECURITY CLASS. (of this report) Unclassified	
		15a. DECLASSIFICATION/DOWNGRADING SCHEDULE	
16. DISTRIBUTION STATEMENT (of this Report) Approved for public release; distribution unlimited			
17. DISTRIBUTION STATEMENT (of the abstract entered in Block 20, if different from Report)			
18. SUPPLEMENTARY NOTES			
19. KEY WORDS (Continue on reverse side if necessary and identify by block number) Atmospheric Density Satellite Cold cathode gauge Particle Flux accumulator			
20. ABSTRACT (Continue on reverse side if necessary and identify by block number) The report contains a description of a U.S. Air Force Geophysics Laboratory Atmosphere Density experiment. Two instruments developed under an earlier program were qualified for space flight and were flown in the spring of 1978. Discussion of instrument performance and flight results are presented.			

DD FORM 1 JAN 73 1473

EDITION OF 1 NOV 65 IS OBSOLETE

UNCLASSIFIED

SECURITY CLASSIFICATION OF THIS PAGE (When Data Entered)

390767

du

TABLE OF CONTENTS

I.	INTRODUCTION	1
II.	GAUGE DESCRIPTION	1
III.	ELECTRONICS DESCRIPTION	3
IV.	BAFFLE OPERATION	3
V.	CALIBRATION DATA	6
VI.	TELEMETRY SYSTEM AND DATA FORMAT	25
VII.	FLIGHT RESULTS	29
VIII.	PERFORMANCE OF ELECTRONIC CIRCUITRY	59
IX.	RECOMMENDATIONS	63
	APPENDIX A	
	Qualification Testing	66

Accession For	
NTIS GSA&I	<input checked="" type="checkbox"/>
DDC TAB	<input type="checkbox"/>
Unannounced	<input type="checkbox"/>
Justification	<input type="checkbox"/>
By _____	
Distributor/	
Availability Codes	
Dist.	Avail and/or special
A	

I. INTRODUCTION

For many years the U.S. Air Force Geophysics Laboratory, Hanscom AFB, MA., has been involved in obtaining upper atmosphere density data using a variety of techniques. Under an earlier program (Air Force Contract No. F19628-74-C-0156) Epsilon Laboratories was responsible for the design and fabrication of two complete satellite density measuring systems utilizing cold cathode gauges as the primary sensor. The systems have been described in detail in an earlier report, (Ref. 1), however, for the benefit of readers of this report a brief description is repeated herein.

Under the provision of a second contract (F19628-76-C-0062), Epsilon Laboratories was responsible to provide further technical assistance, provide any refurbishment as required and conduct the necessary qualification tests prior to flight.

The report describes the results of a satellite experiment launched in the spring of 1978. Although the instruments operated without any known failure, anomalies do exist between the cold cathode gauge and particle flux accumulator experiments. Using the pertinent laboratory calibration data the flight data has been reduced and evaluated. Finally, several recommendations are made for a future program of this type.

II. GAUGE DESCRIPTION

The principle of the cold cathode gauge derives from the so-called Penning gauge. This class of sensors does not require a hot filament as do conventional type ionization gauges. The cold cathode gauge consists of two electrodes separated by a cylindrical or ring shaped anode located in an axial magnetic field. A potential of several thousand volts is applied between the electrodes. The electrons produced in the gas discharge oscillate in spiral paths between the cathodes producing an ion current which can then be related to pressure which in turn can be related to ambient density.

The gauges (Model 529) utilized in the measurement were fabricated by the Cabot Corporation, Billerica, Massachusetts. These are lightweight (less than 3 lbs.), low power sensors with a dynamic range of 1×10^{-4} Torr to 10^{-10} Torr and were originally designed for the Apollo 12 through 15 missions. Later a version was flown on a U. S. Air Force Satellite, the OV1-15. Figure 1 illustrates the gauge as modified for the present program. In particular, several baffle plates originally located within the mouth of the gauge (for the purpose of reducing photon sensitivity, charge particles and dust) were removed to permit a higher vacuum conductance in the present application. The overall accuracy of the gauge is specified at $\pm 20\%$ from 1×10^{-4} Torr to 10^{-8} Torr with correspondingly less accuracy at lower pressures. Gauge sensitivity is known to be a function of the anode voltage ranging from 0.5 Amp/Torr at 1250 volts to 1 Amp/Torr at 1700 volts.

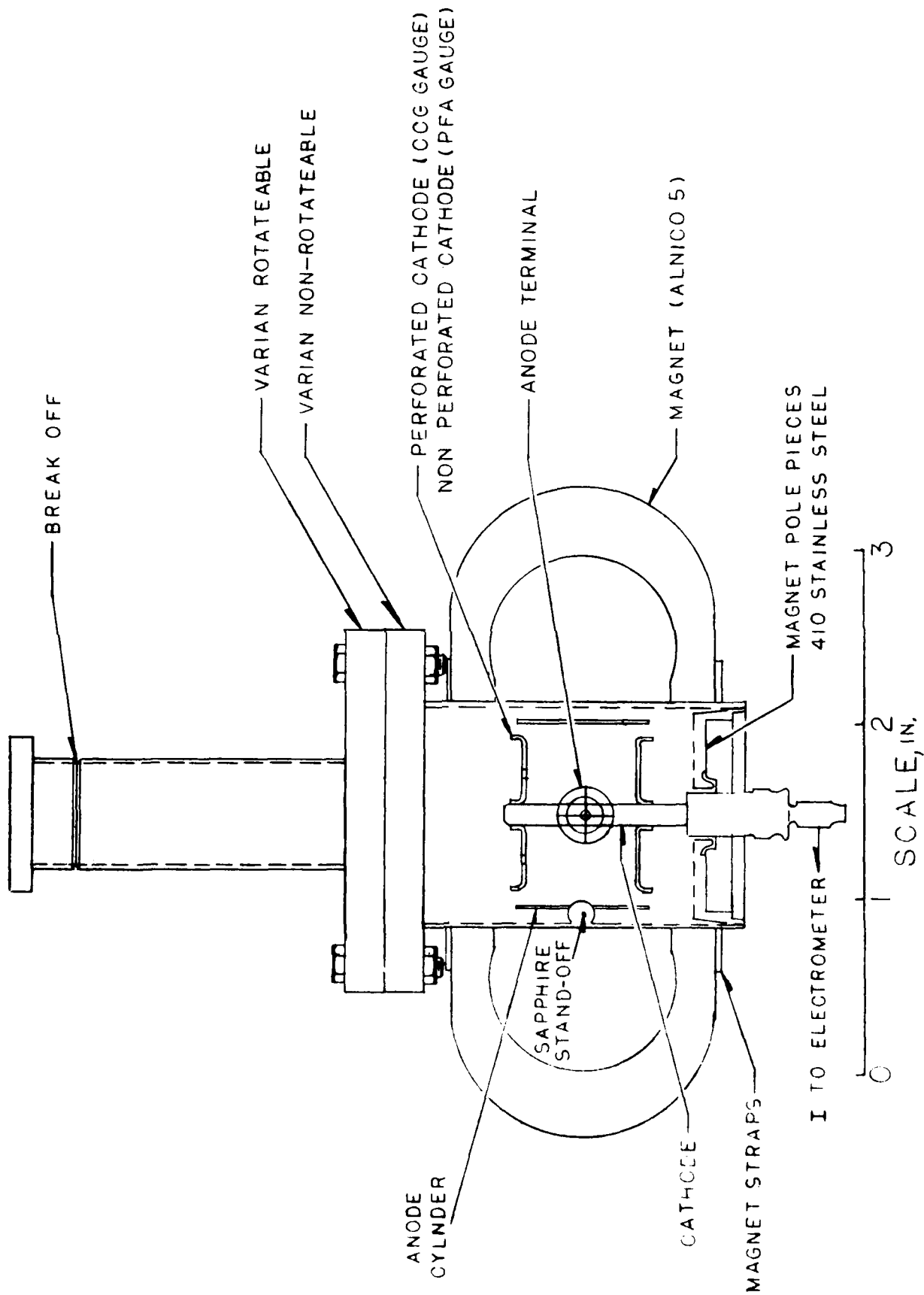


Figure 1 SCHEMATIC OF THE COLD-CATHODE
MAGNETRON PRESSURE GAUGE

The two systems fabricated and launched in the S3-4 satellite payload each incorporate cold cathode gauges as the sensing element. One, designated the cold cathode experiment CCG and the second called the PFA (particle flux accumulator) serve to measure atmospheric density and its variation. This data is used to upgrade and refine existing Air Force Atmospheric models and also is useful in the investigation and study of the mechanism and energy sources by which variations (diurnal, semi-annual, annual, geophysical and solar effects) are propagated (Ref. 2,3). The sensors are initially sealed and opened to the atmosphere by a pyrotechnic device after the satellite has achieved orbit. Atmospheric gas flows into the sensor cavity creating an internal gauge pressure from which the density is obtained after correcting for factors such as temperature and gauge aspect angle.

III. ELECTRONICS DESCRIPTION

Each system consists of two separate packages, one housing a cold cathode gauge, mechanical baffle arm, baffle circuitry and high voltage power supply. The second package contains the electrometer amplifier, power supply and buffer circuitry. The signal processing portion of the system consists of an integrated circuit logarithmic amplifier and 0-5 VDC buffer circuitry for translating the gauge pressure to a TM compatible signal. The gauge high voltage supply is encapsulated in the gauge housing to reduce potential breakdown hazards. The high voltage is attenuated and monitored via buffer circuits through the TM and provides an inflight confidence check of proper gauge anode voltage. Temperature of both the gauge and electronic boxes are monitored by means of a sensistor operational amplifier circuit. The gauge sensistor (temperature sensitive element) is mounted on the support structure while the electronic box sensistor is mounted on the electrometer circuit board. Both provide ambient temperature data to the TM for data evaluation. The gauge open monitor circuit provides a confidence check that the tubulation breakoff pyrotechnic devices have fired and exposed the gauge inlets to the ambient atmosphere. Inflight electrometer calibration is accomplished by automatically switching the electrometer input from the gauge to an exponential decaying precision current approximately once every 50 seconds. A filter regulator, inverter circuit provides +28 VDC, +15VDC and +5 VDC for system operation. The regulator has short circuit and reverse polarity protection.

The two photographs shown in Figures 2 and 3 illustrate the various components which make up a complete PFA system; the CCG is identical except for the mirror image placement of the baffle.

IV. BAFFLE OPERATION

A baffle extension was incorporated as a secondary mode of operation of the PFA and CCG systems. This mode of measurement consisted of extending and retracting a plane baffle arm fabricated of brass (see Figures 2,3) parallel to the gauge axis which interrupt the transport of particles into the gauge creating a signal dropout. The resulting decrease in gauge

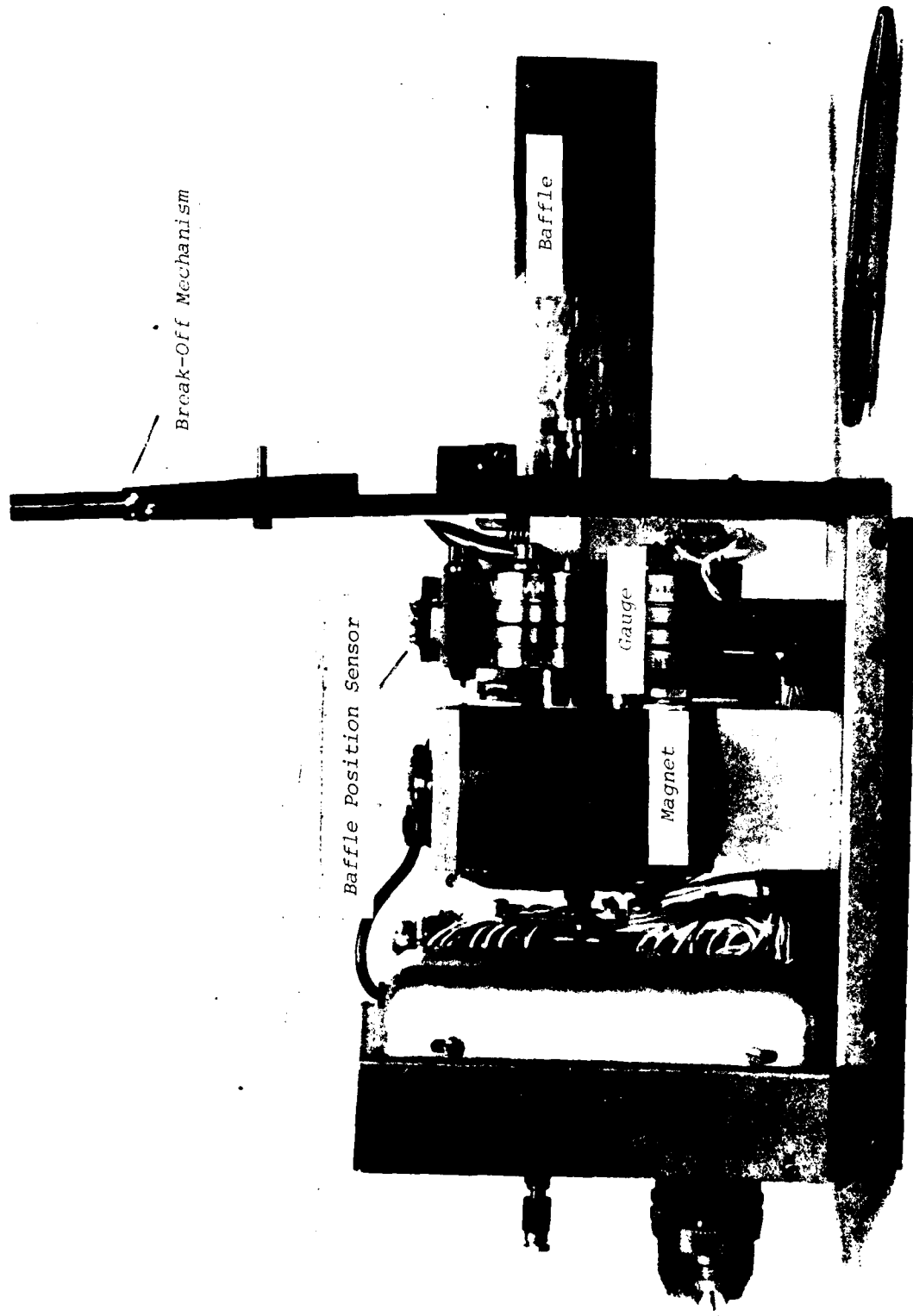


Figure 2 PFA Gauge System

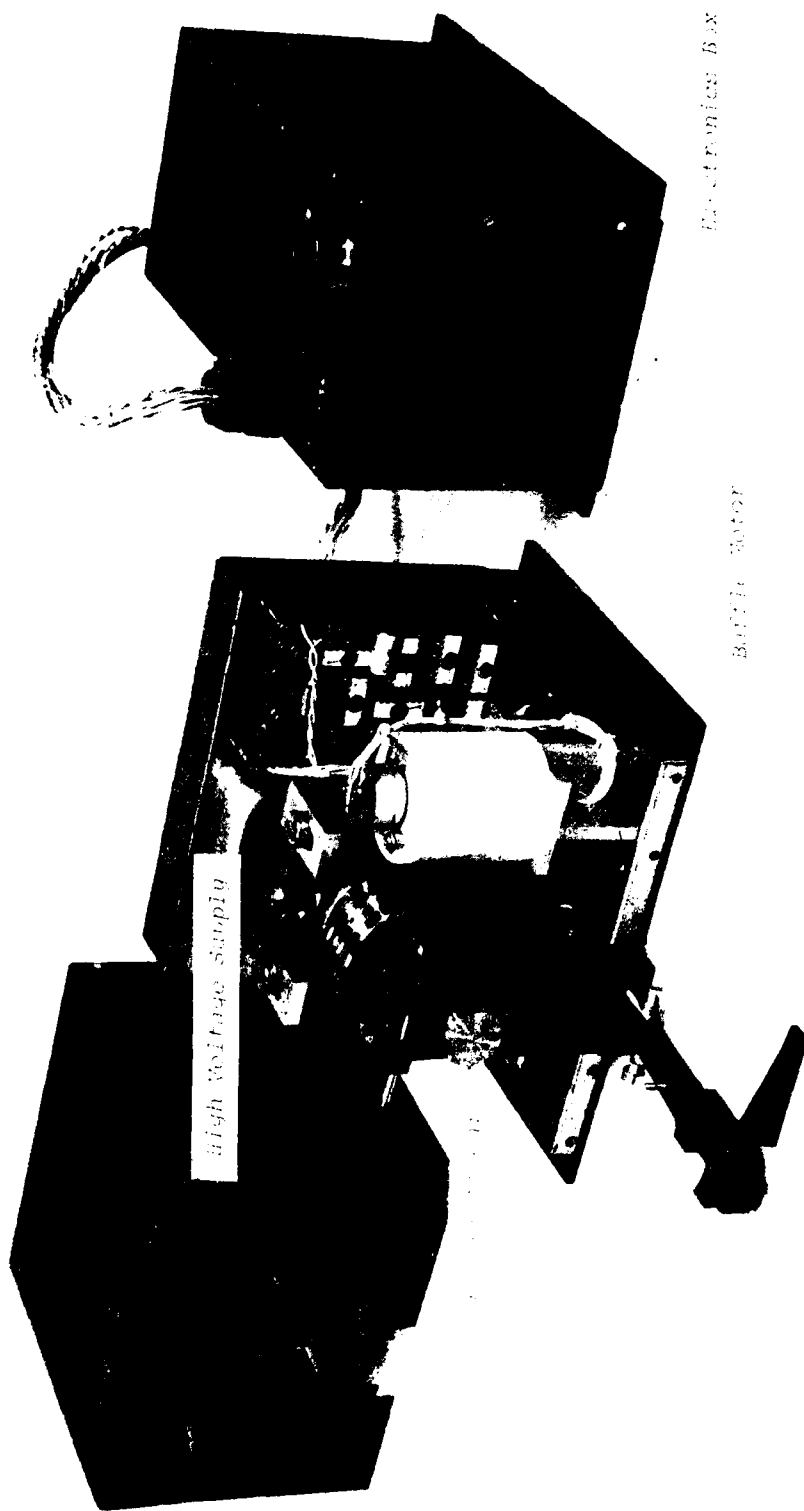


Figure 3 PFA Gauge System

ion current as a function of baffle extension combined with the known geometric configuration may be used to determine the aspect angle between the gauge sensitive axis and the velocity vector.

The baffle arm was coiled inside a white teflon housing and operates analogous to a carpenter's tape measure. When a baffle extend command is initiated, a stepping motor shaft moves an inner teflon housing on which the baffle is mounted and coiled, extending the baffle arm. When the baffle arm reaches maximum extension it trips an optical limit switch which initiates a baffle retract command. The baffle then retracts till it trips an optical limit switch at its stowed position. The baffle arm then waits in this stowed position until it again receives a baffle extend command. When the gauge system is either turned on or off the baffle will always be commanded to retract to its stowed position should it be in an extended position.

The baffle housing was mechanically mounted such that an extension would be symmetrical about the gauge at a precisely measured distance from the gauge. A monitor of baffle extension was obtained by mechanically coupling the baffle arm to a precision servo potentiometer which generated a D-C voltage proportional to baffle extension. The infrared photooptical sensor monitored the position of a reflecting strip attached to the teflon drum which advances the baffle outward and inward.

V. CALIBRATION DATA

In order to reduce the flight data the pre-launch system calibration measurements are required. In this regard we have included the necessary information to reduce the various data outputs including currents, high voltage monitors, equipment temperature monitors and baffle deployment monitors for both instruments.

a) Pressure Calibration

Figures 4 and 5 represent the CCG and PFA gauge calibrations and illustrates the equivalence of the two gauges over practically the entire range from 10^{-9} Torr to 10^{-4} Torr. The plots are extracted from the original data provided by F. Torney, Cabot Corporation. The primary pressure standard was a Bayard-Alpert gauge traceable to the AVCO Corporation, Wilmington, MA. Table 1 permits a quick comparison of the two gauges at several discrete pressures. Although some differences are noted presumably the reduction to atmospheric density utilizes a least squares fit to both of the pressure/current curves of Figures 4 and 5.

b) Gauge High Voltage Calibration

The gauge high voltage monitor may be reduced through the use of Figures 6 and 7. The operating voltage of the two instruments was set to 1800 Volts during pre-launch corresponding to monitor outputs of 3.54 Volts for the CCG and 3.8 Volts for the PFA.

GAUGE CALIBRATION DATA USING BAYARD-ALPERT
IONIZATION GAUGE AS STANDARD

<u>Pressure</u>	<u>PFA GAUGE Current</u>	<u>CCG GAUGE Current</u>	<u>Ratio PFA/CCG</u>
1×10^{-4} Torr	4×10^{-5} Amp	4.7×10^{-5} Amp	.851
5×10^{-5} Torr	2.8×10^{-5} Amp	2.8×10^{-5} Amp	1.00
1×10^{-5} Torr	7×10^{-6} Amp	8×10^{-6} Amp	.875
5×10^{-6} Torr	4×10^{-6} Amp	4.7×10^{-6} Amp	.851
1×10^{-6} Torr	9×10^{-7} Amp	1.05×10^{-6} Amp	.857
5×10^{-7} Torr	4.5×10^{-7} Amp	5.7×10^{-7} Amp	.789
1×10^{-7} Torr	1×10^{-7} Amp	9.5×10^{-8} Amp	1.053
5×10^{-8} Torr	5×10^{-8} Amp	4.3×10^{-8} Amp	1.16
1×10^{-8} Torr	8.8×10^{-9} Amp	5.5×10^{-9} Amp	1.6
5×10^{-9} Torr	4.2×10^{-9} Amp	2.8×10^{-9} Amp	1.5
1×10^{-9} Torr	6.4×10^{-10} Amp	3.7×10^{-10} Amp	1.729
5×10^{-10} Torr	9.6×10^{-11} Amp	4.0×10^{-11} Amp	2.4

TABLE 1

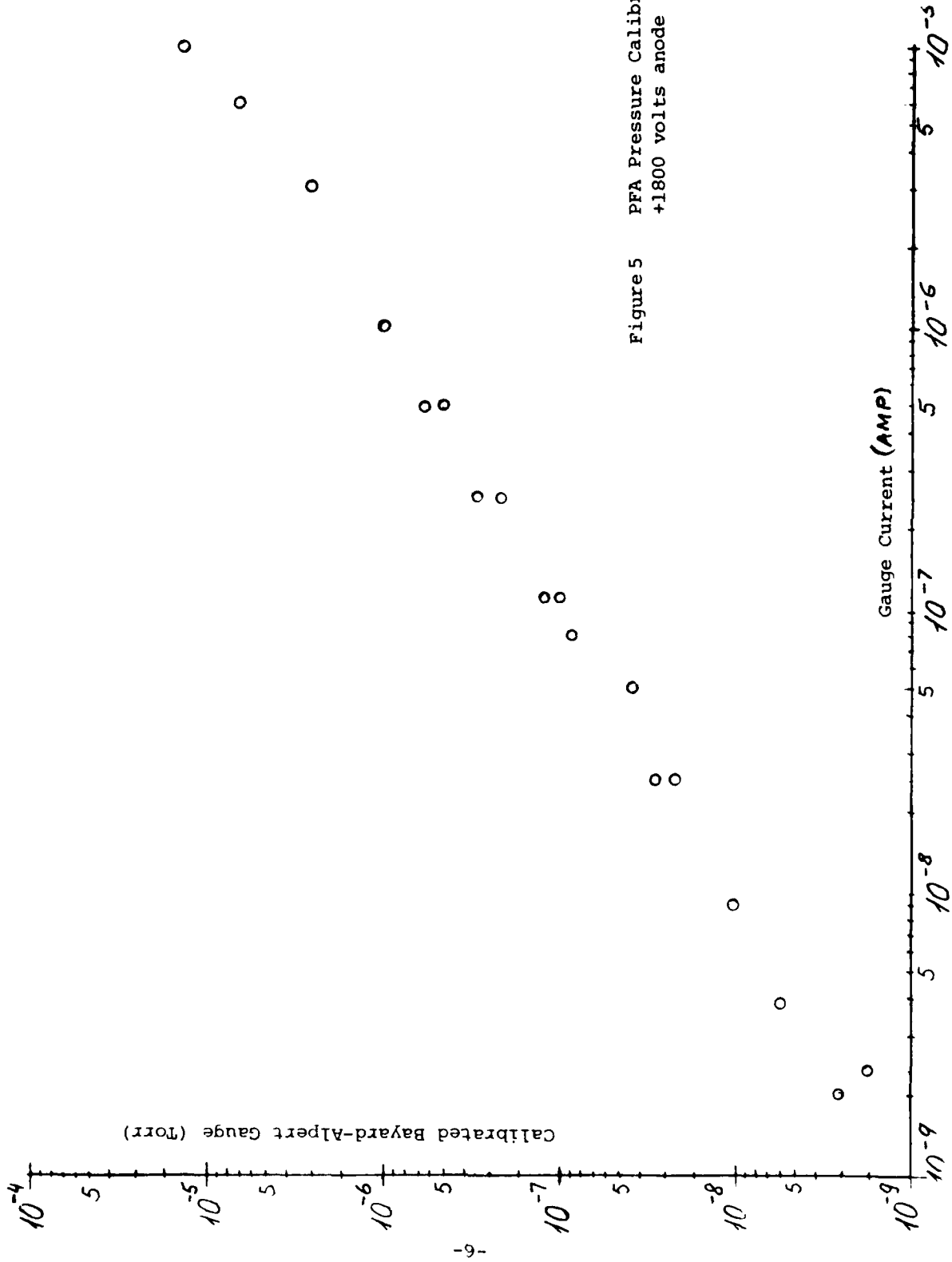
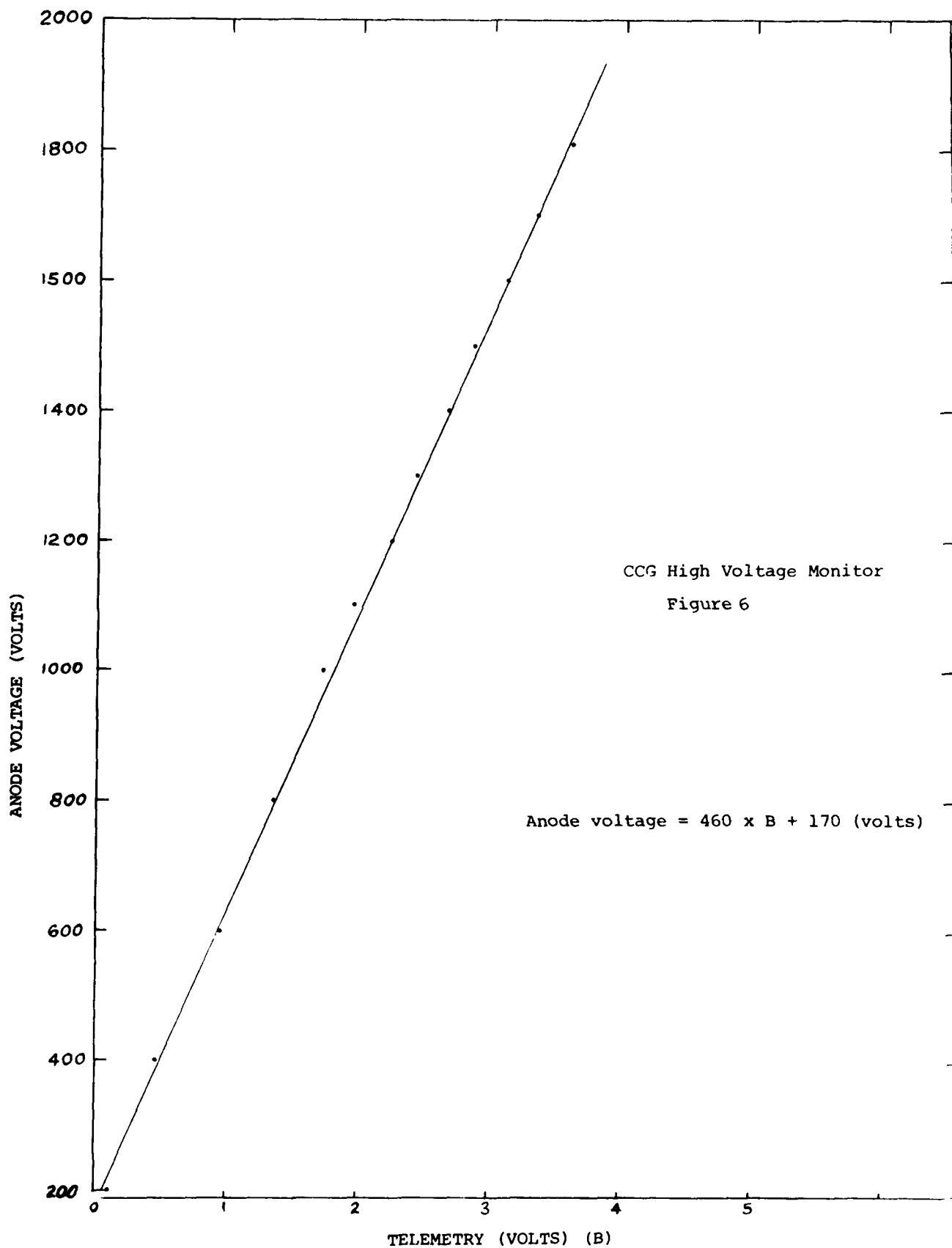
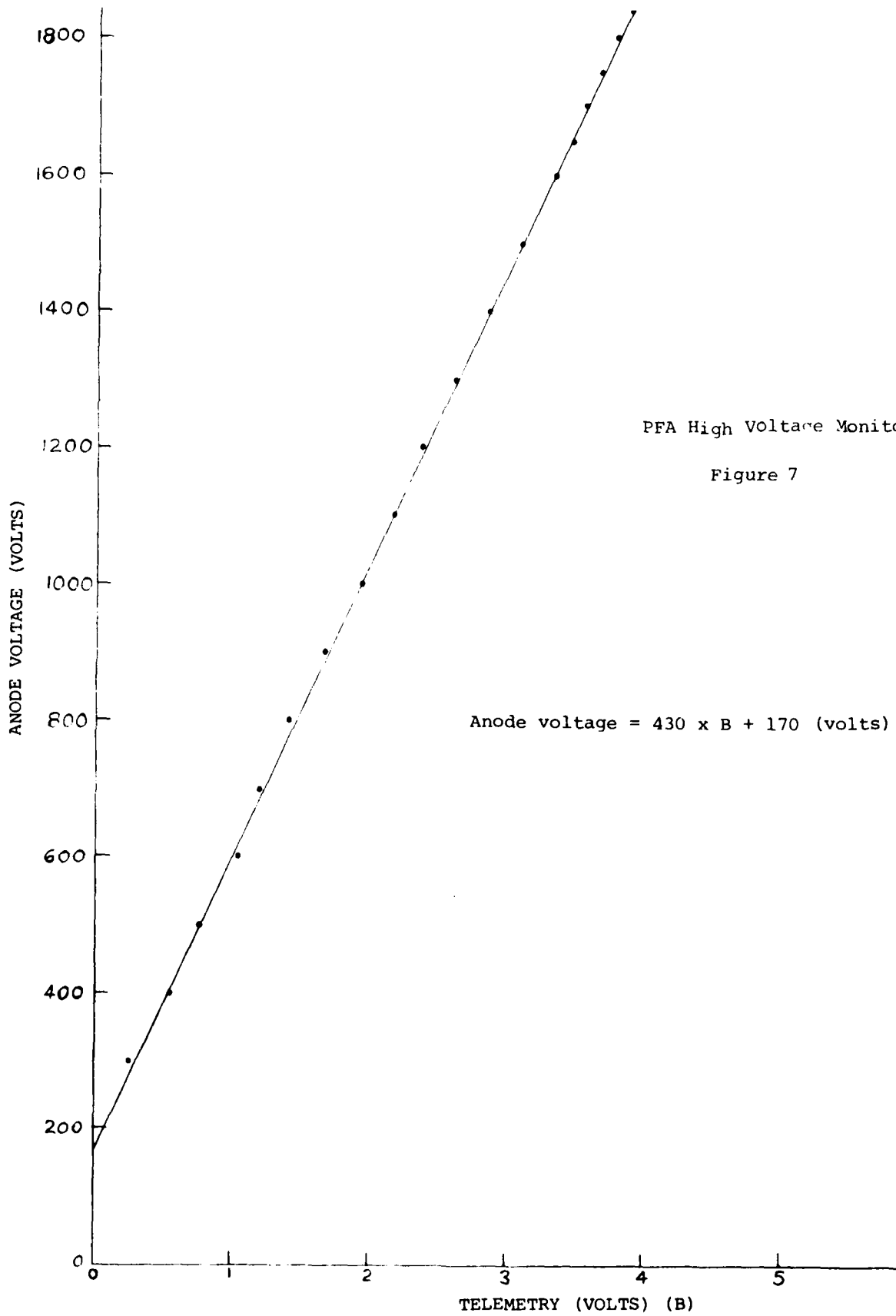


Figure 5 PFA Pressure Calibration
+1800 volts anode





c) Baffle Calibration

Prior to launch both instruments were dimensionally checked in order to establish an accurate relationship between the physical extension of the baffles and the potentiometer monitor. Figures 8,9 illustrate the placement of the break-off point on each of the gauges with respect to the baffle location. These data together with the measured potentiometer outputs at minimum and maximum extension yield the equations shown in Figures 8,9. Additionally, the straight lines represented by these equations are included in Figures 10,11.

d) Temperature Calibration

Temperature sensors were installed in both the gauge housing and electronics boxes to permit an evaluation of thermal effects should any have occurred in flight. Figure 12 represents a typical calibration run for the CCG electronics performed in the laboratory in order to determine the temperature response of the log amplifier. It is to be noted that virtually no difference in operation was observed between -20°C and $+22^{\circ}\text{C}$. The curves shown in Figures 13,14 represent the thermistor calibrations to be used in conjunction with the temperature monitors for each instrument.

e) Current Calibration

The most significant data outputs in the experiment, of course, are those providing the actual current measurements from each instrument. In order to ensure system performance was maintained an internal calibration was exercised over the entire duration of the satellite experiment. This calibration sequence permits frequent checks to ascertain that the dc calibrations illustrated in Figures 15,16 are holding true. In this regard it is worthwhile to understand the operation of the in-flight automatic calibration sequence.

The auto calibration sequence for the PFA and the CCG instruments occurs approximately every 50 seconds. During each calibration sequence a relay circuit switches off the normal signal input current to each electrometer amplifier and a controlled time varying source of calibration current is provided instead.

The first tenth of a second of the calibration sequence consists of supplying a constant level of .99 microamperes to the input of each electrometer thereby providing a convenient "mid-scale" calibration point. The .99 microampere level is large enough to exercise the bottom end of the density output amplifier and small enough not to saturate the range output amplifier. At time, T_0 , which corresponds to the end of the first tenth second of calibration, a second relay circuit removes the .99 microampere constant current source and replaces it with the current provided by a capacitor, C_0 , which is discharged into the electrometer input through a $150\text{ K}\Omega$ current limiting resistor, R_0 . Because the electrometer input is

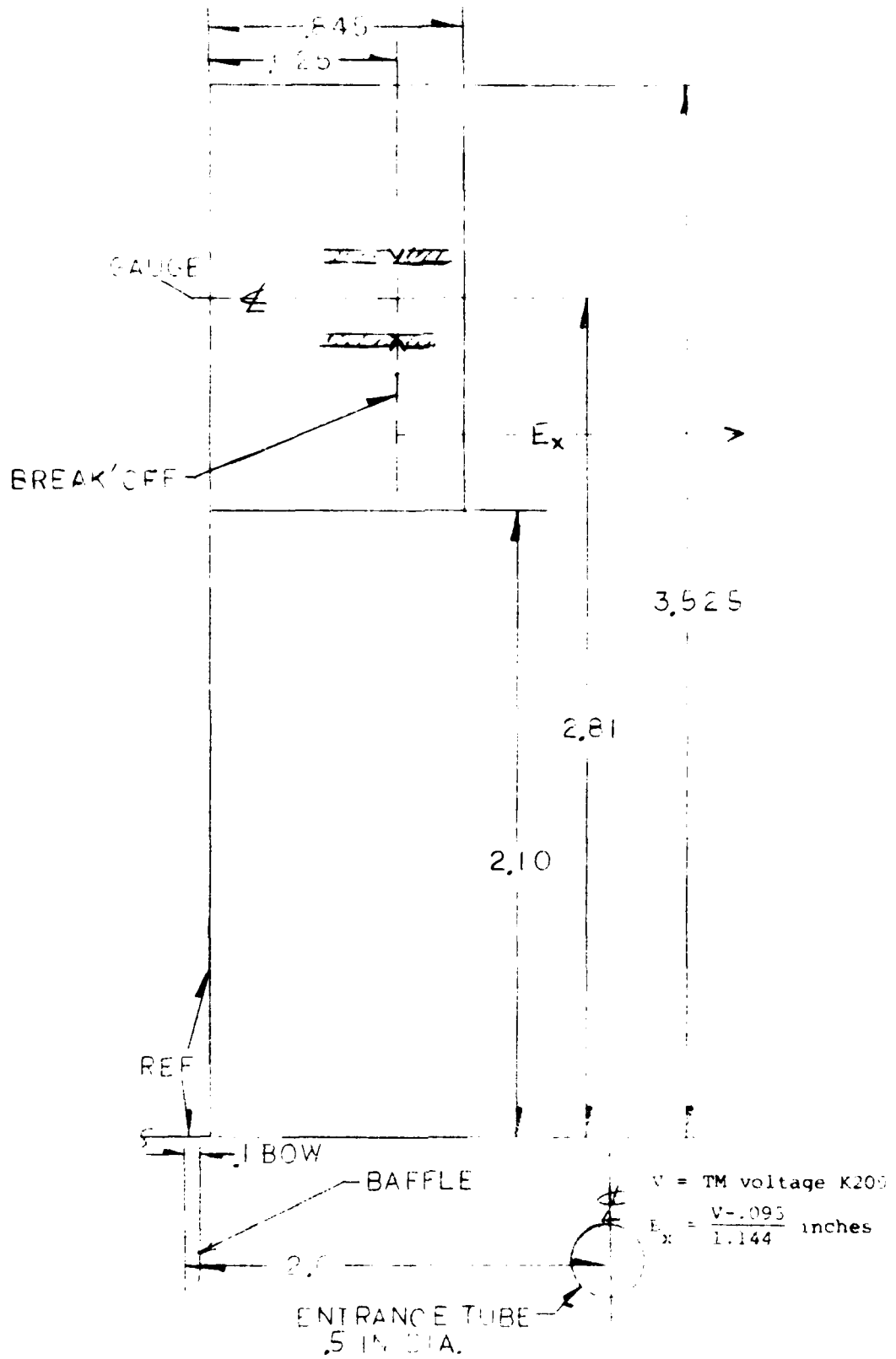


Figure 8 Critical Baffle Dimensions

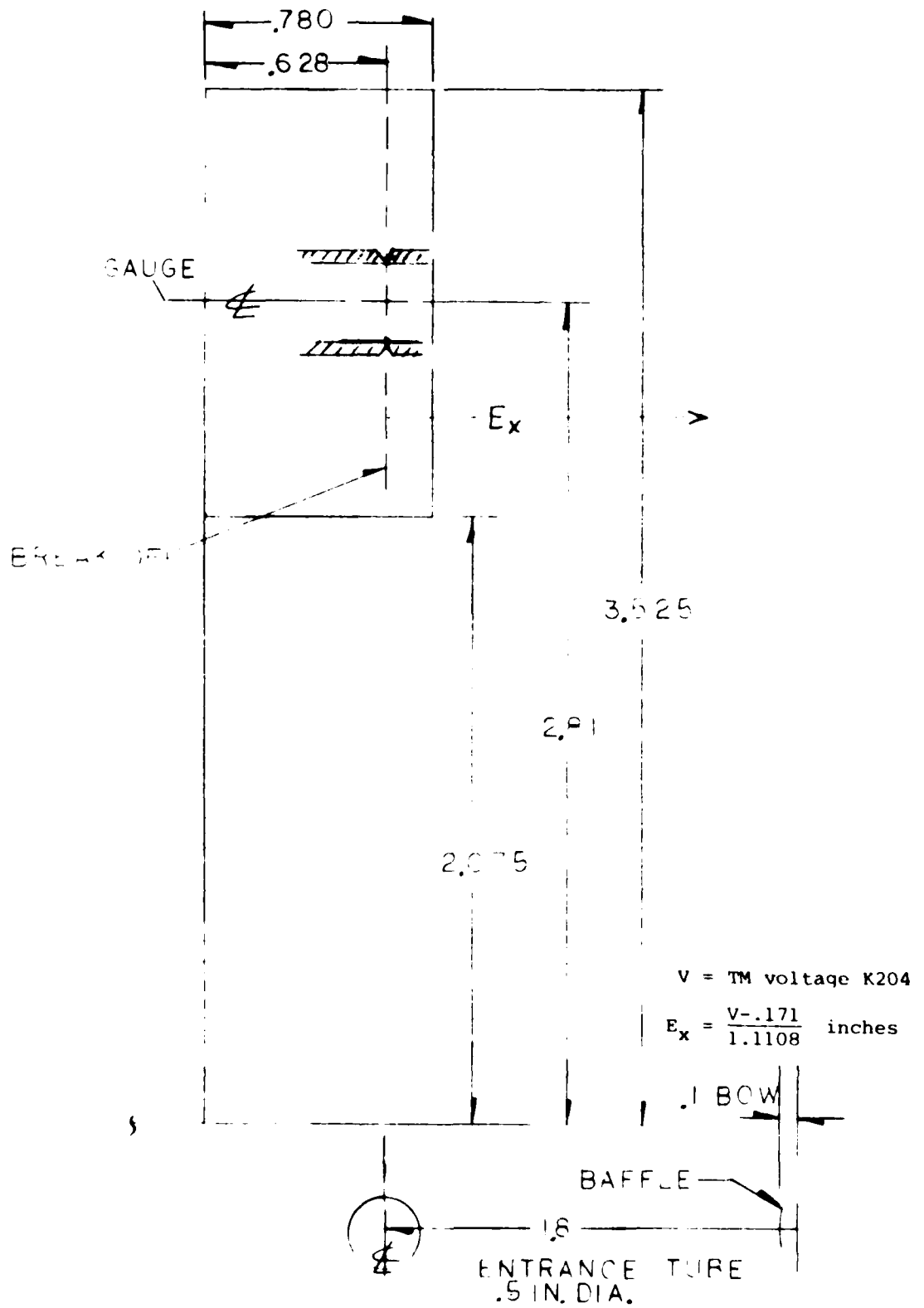


Figure 9 PFA Critical Baffle Dimensions

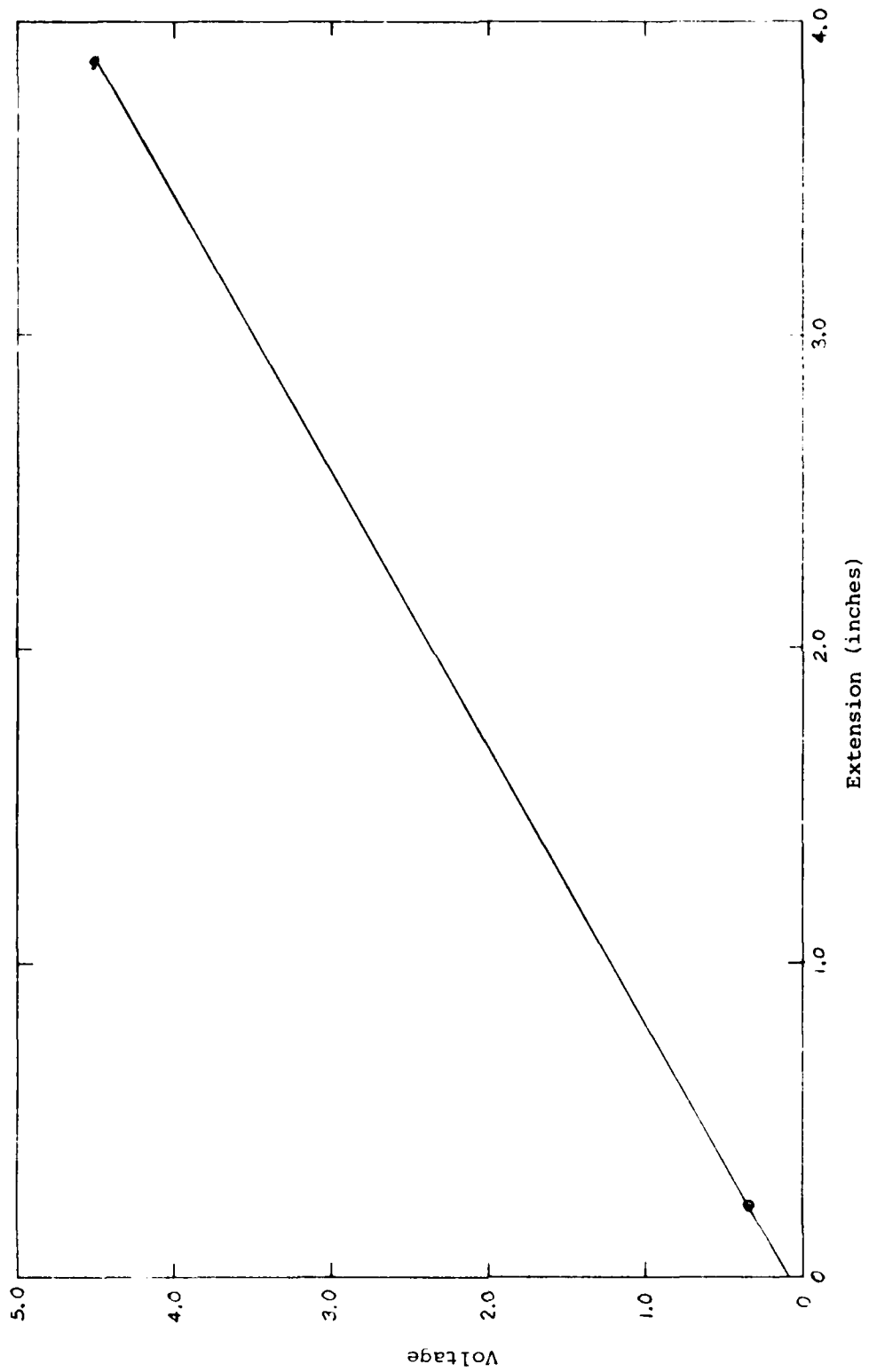


Figure 10 CCG Baffle Extension Calibration

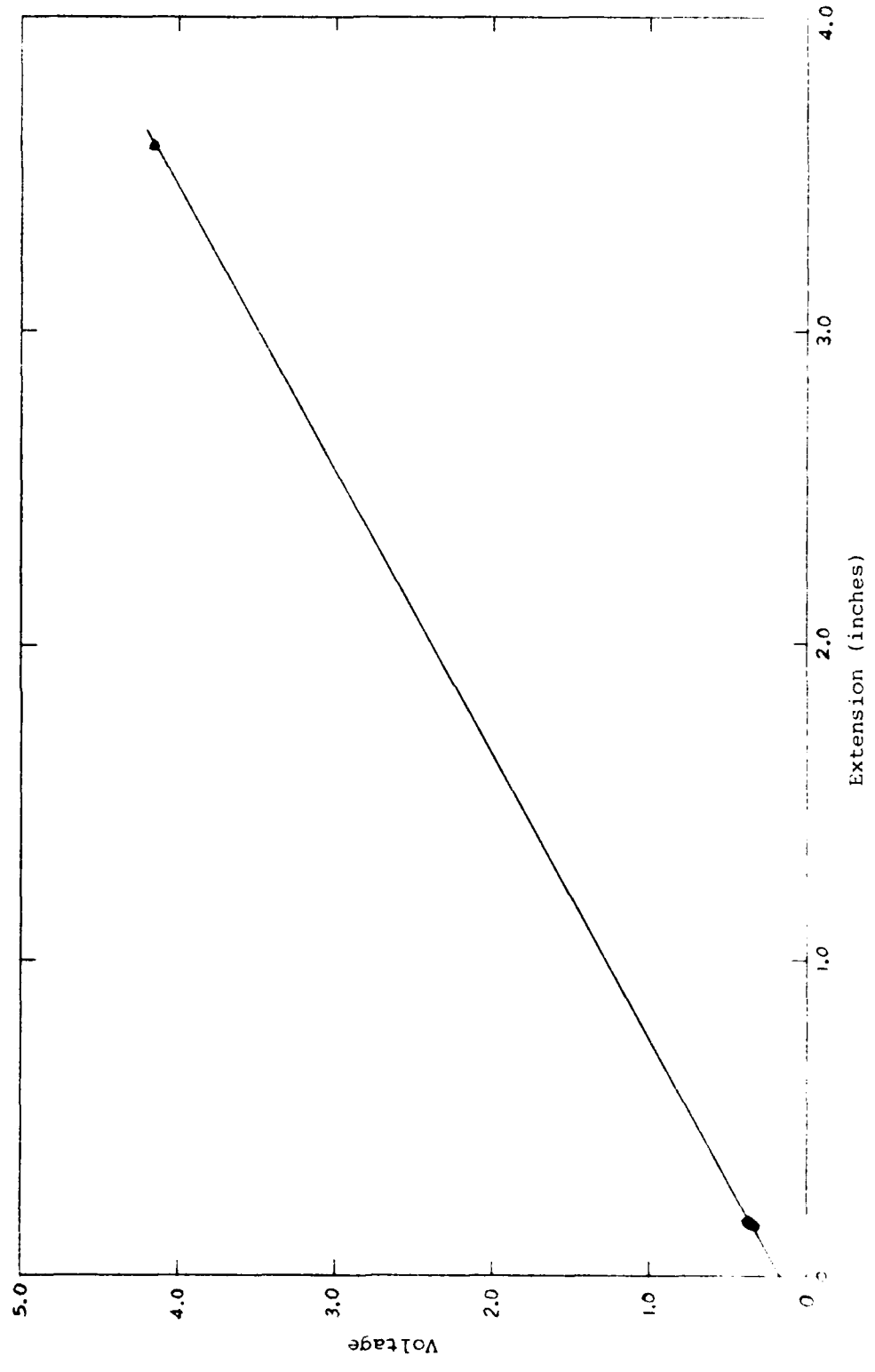


Figure 11 PFA Baffle Extension Calibration

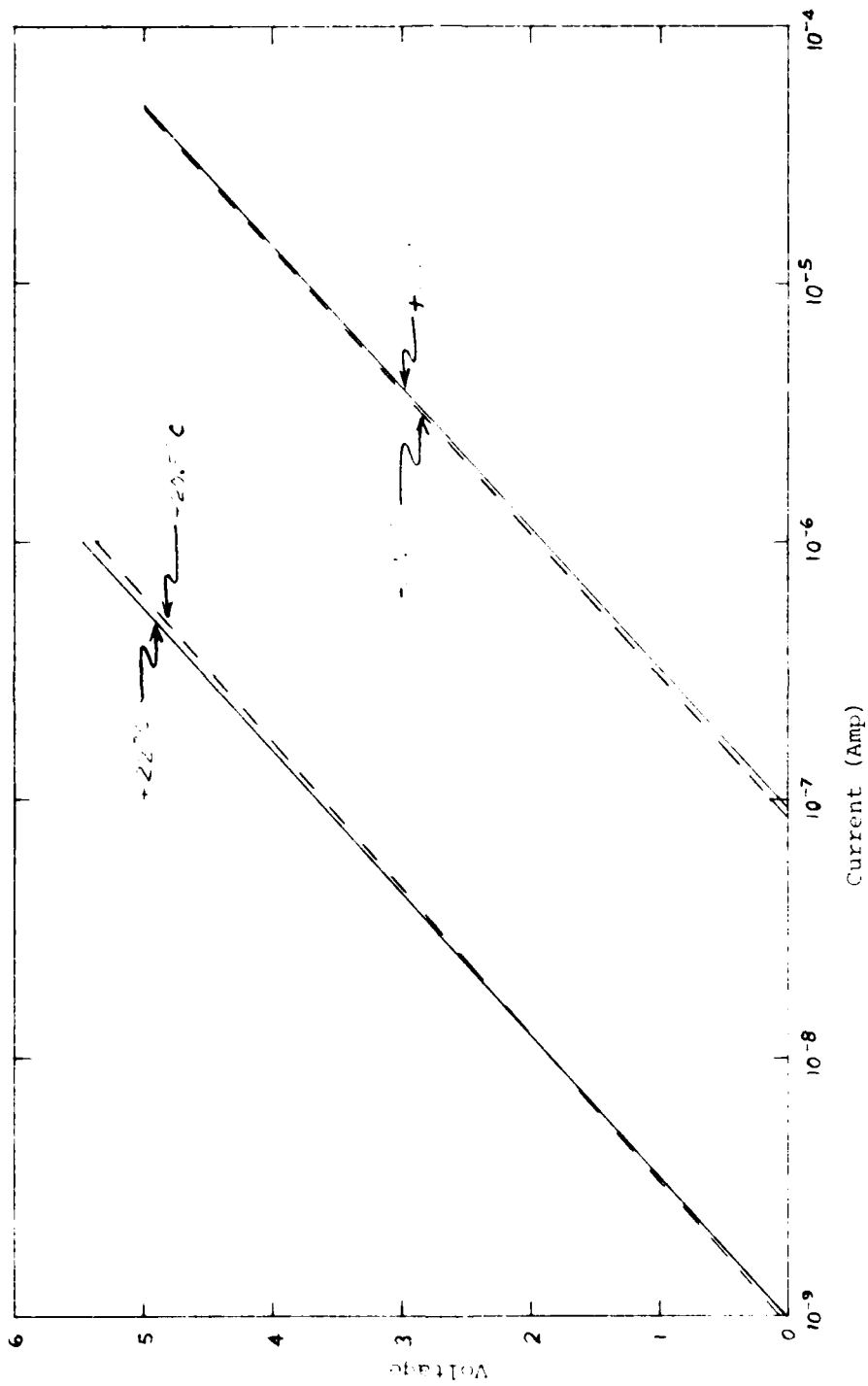


Figure 12 CCG Electronics Temperature Calibration

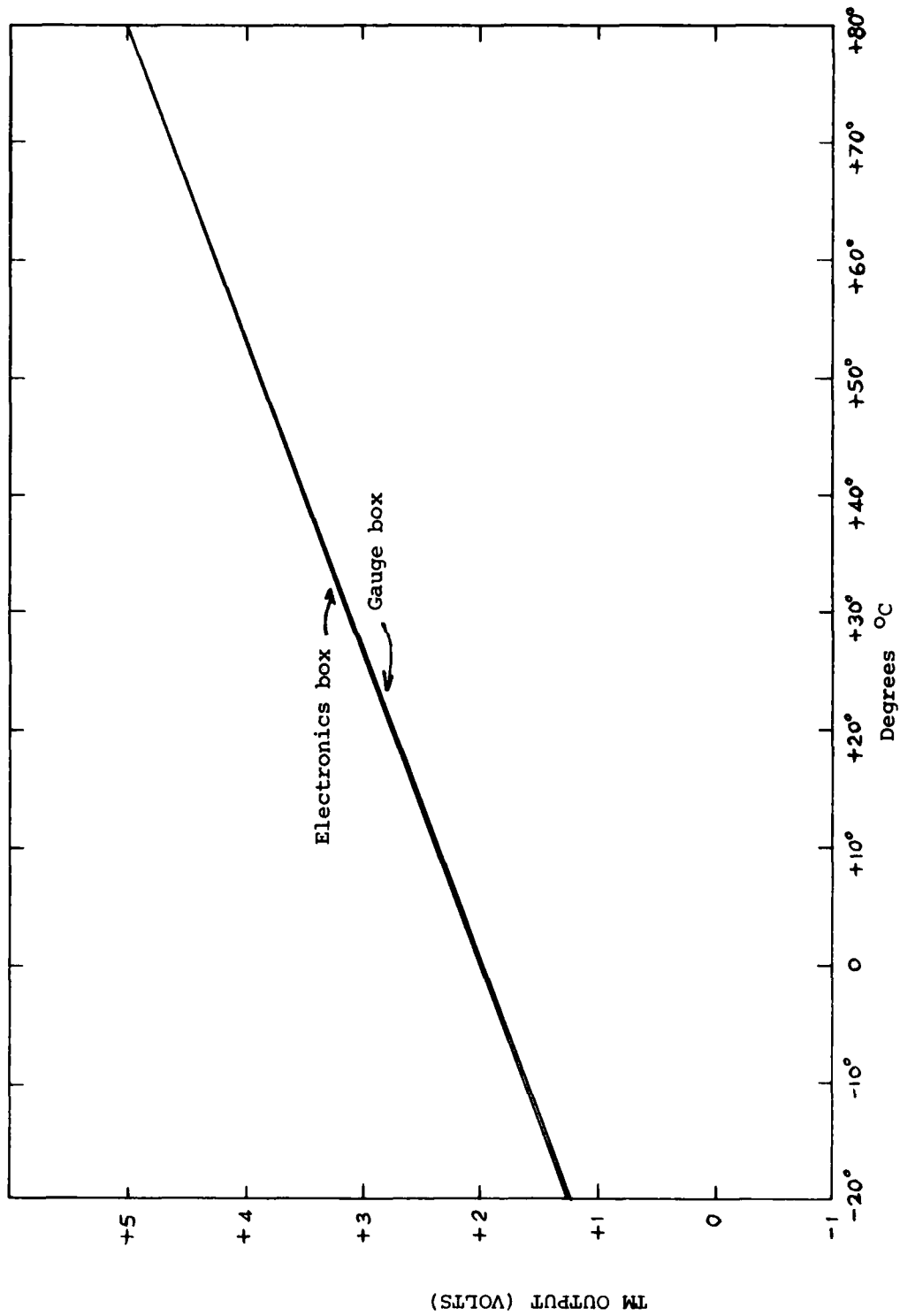


Figure 13 Temperature Monitor - CCG System

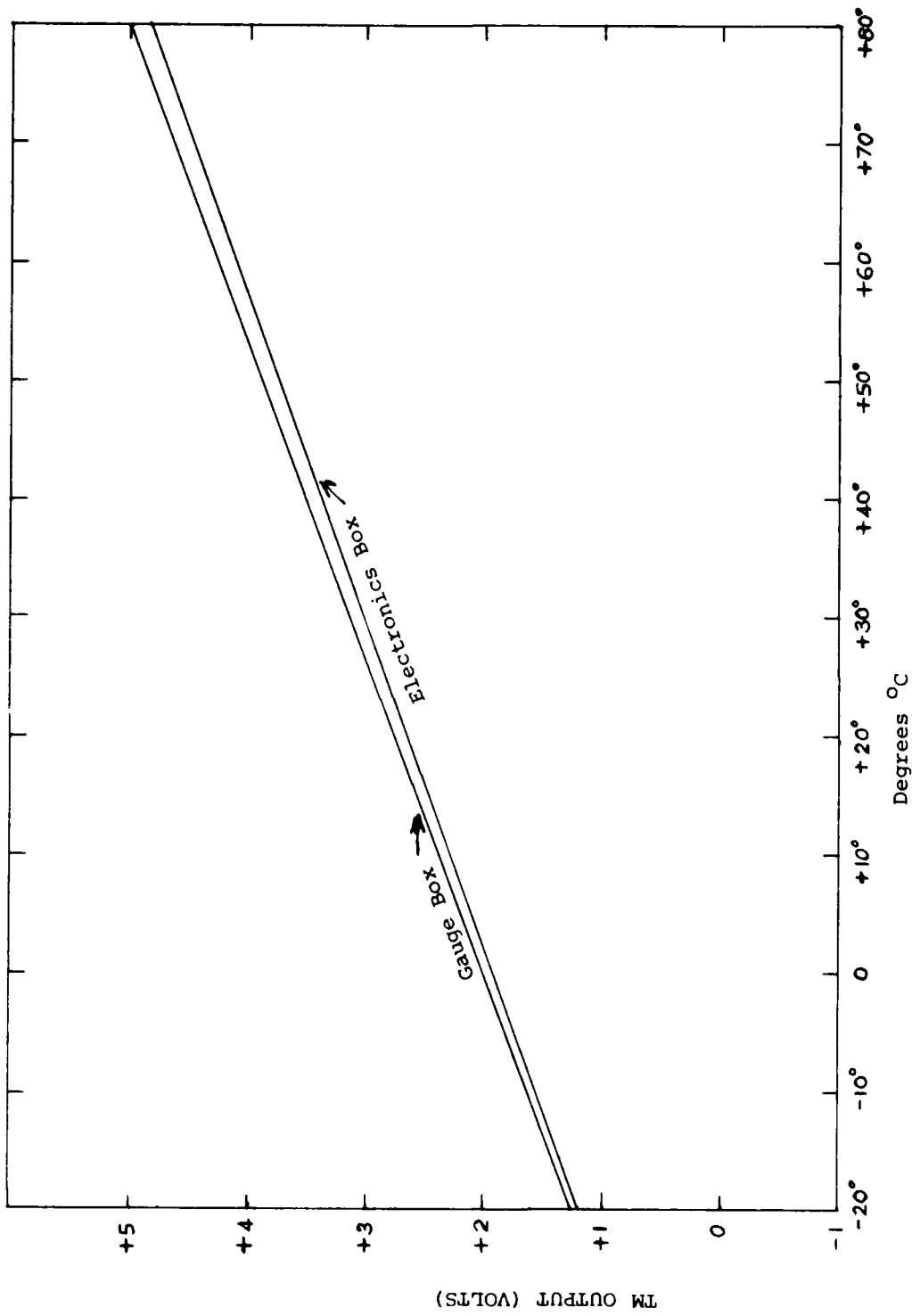


Figure 14 Temperature Monitor - PFA System

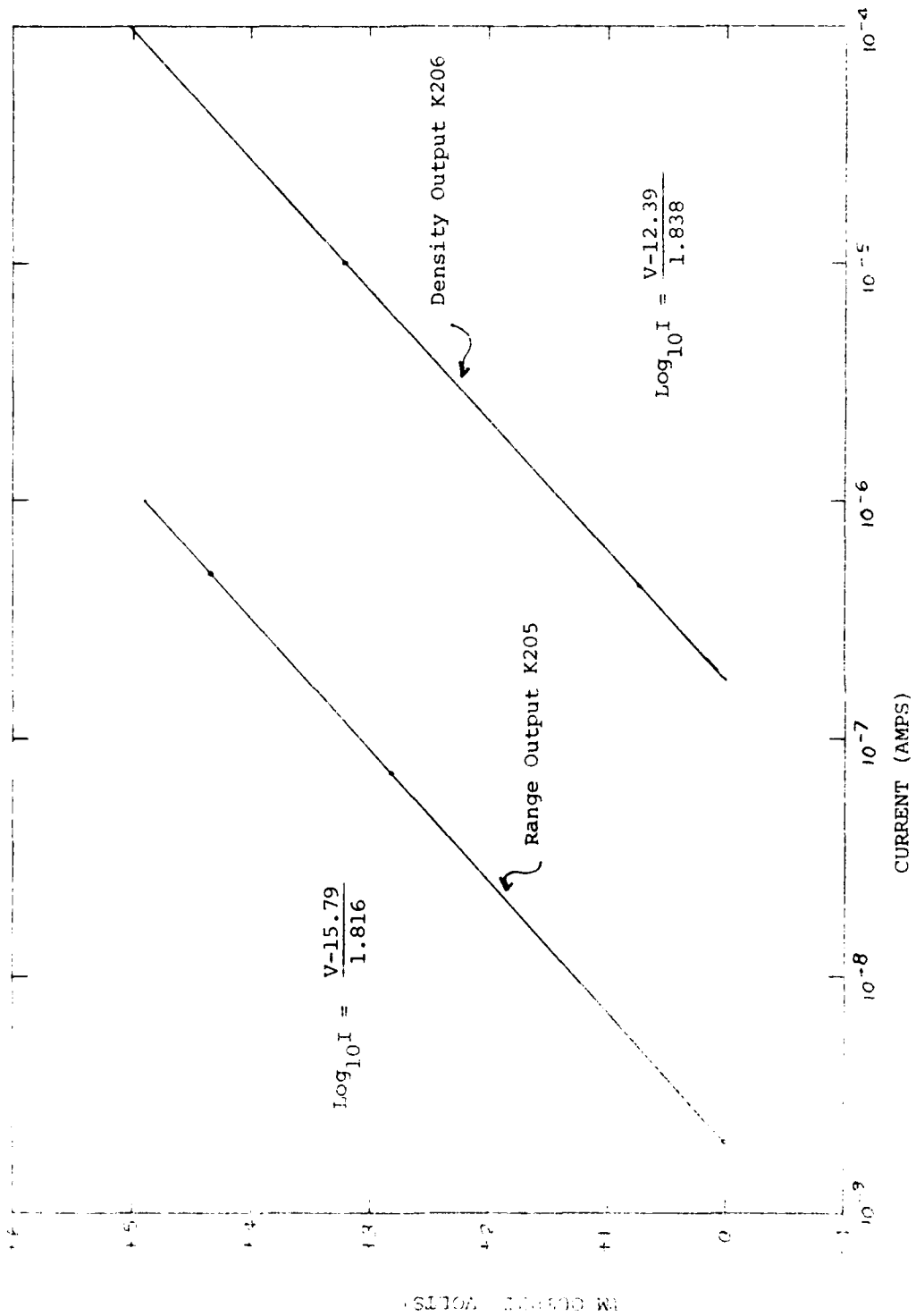


Figure 15 CCG Analog output voltage vs. gauge current

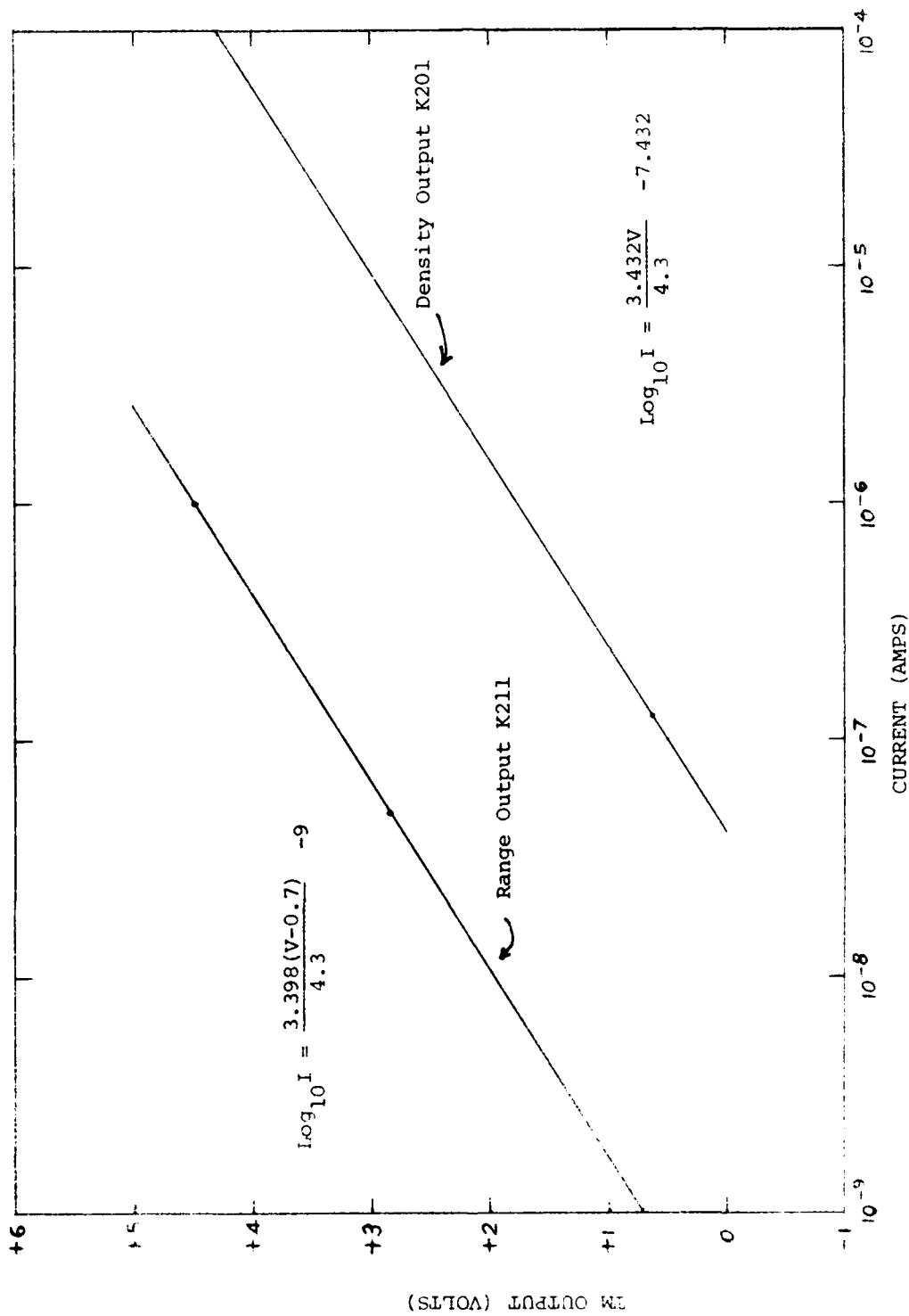


Figure 16 PFA Analog output voltage vs. gauge current

held at a virtual ground potential, the input current to the electrometer will be given by

$$I_{cal} = \frac{V_{co}}{R_o} e^{-\frac{(T-T_0)}{\tau}} = \frac{15}{150 \times 10^3} e^{-\frac{(T-T_0)}{\tau}}$$

$$I_{cal} = 1.00 \times 10^{-4} e^{-\frac{(T-T_0)}{\tau}}$$

Where $\tau = R_o C_o = .15$ sec nominal and V_{co} is the initial voltage across C_o . The design value of V_{co} is $15V \pm 1\%$.

During this decaying portion of the calibration sequence the outputs of the logarithmic amplifiers will be the linear responses indicated in Figure 17. Because of the large range of current inputs provided, excessively large errors could be introduced in the determination of calibration levels if the parameters τ and T are directly inserted into the above equation, e.g., by an automatic computer program which would generate the sequence of values of I_{cal} . The error problem arises both from errors in parameter values and errors in time determination.

Processing of Calibration Signals

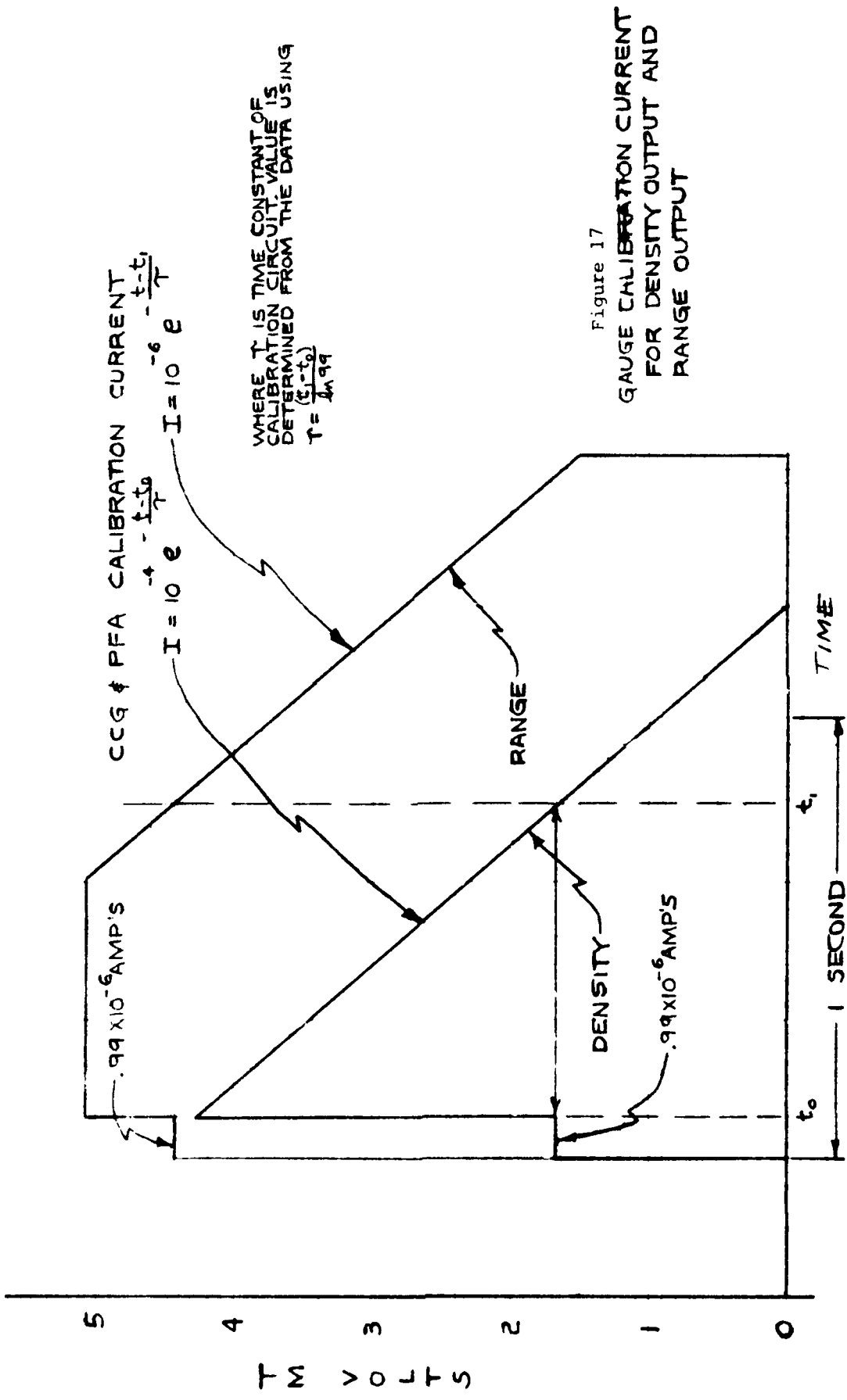
Although all the parametric (C_o, V_o, R_o) elements which affect I_{cal} are quite accurate and stable except for the determination of the initial value of C_o , considerable error multiplication can result from relatively minor changes in the values of C_o and R_o because of the large dynamic range of the calibration current input levels. The estimated error, obtained by differentiating the equation of I_{cal} , gives

$$\frac{\Delta I_{cal}}{I_{cal}} = \frac{\frac{\partial I_{cal}}{\partial V_{co}} \Delta V_{co} + \frac{\partial I_{cal}}{\partial R_o} \Delta R_o + \frac{\partial I_{cal}}{\partial C_o} \Delta C_o}{I_{cal}}$$

$$\frac{\Delta I_{cal}}{I_{cal}} = \frac{\Delta V_{co}}{V_{co}} + \frac{\Delta R_o}{R_o} \left(\frac{t}{\tau} - 1 \right) + \frac{t}{\tau} \frac{\Delta C_o}{C_o}$$

The system accuracies are such that both $\frac{\Delta V_{co}}{V_{co}}$ and $\frac{\Delta R_o}{R_o}$ are each less than 1% so that the error will primarily be given by

$$\frac{\Delta I_{cal}}{I_{cal}} = \frac{t}{\tau} \left(\frac{\Delta R_o}{R_o} + \frac{\Delta C_o}{C_o} \right)$$



WHERE T IS TIME CONSTANT OF CALIBRATION CIRCUIT. VALUE IS DETERMINED FROM THE DATA USING $T = \frac{(t_1 - t_0)}{.99}$

Figure 17
GAUGE CALIBRATION CURRENT FOR DENSITY OUTPUT AND RANGE OUTPUT

It can thus be seen that the error in the determination of calibration current builds up linearly with time. Fortunately, however, the error can be largely eliminated by determining the time, T_1 , at which time the exponentially decaying I_{cal} input is just equal to the "mid-range" level provided during the first 0.1 second of the calibration interval. At this point

$$I_{cal} = .99 \times 10^{-6} = 1.00 \times 10^{-4} e^{-\frac{(T_1 - T_0)}{\tau}}$$

It can thus be seen that the error in τ can "essentially" be calibrated out by solving for τ in the above equation.

Unfortunately, the determination of the exact time corresponding to T_1 and T_0 is not as direct as one would have desired as a consequence of the 1/32^o second sampling time resolution of the telemetry system. However, the following procedures can be used to obtain a reasonable accurate interpolated value for T_1 and a somewhat less accurate estimated value for T_0 .

The procedure for determining T_1 and T_0 consists of first plotting the two curves in Figure 1 using the telemetered flight data obtained during the calibration interval and noting the exact temporal location of each 1/32 second sampling point. To determine T_1 , locate that point on the decaying portion of the density curve which has the same ordinate value as the ordinate value during the initial 0.1 second of the calibration interval, i.e., the density output value for a current input of $.99 \times 10^{-6}$ amperes. When this has been done, note the relative time position of this point relative to the two adjoining 1/32 second sampling points and perform the appropriate linear interpolation in order to obtain a corrected value of incremental time. This increment should then be added to the time corresponding to that 1/32 second sampling point which just precedes the above equality condition.

The determination of T_0 is less well defined because of the fact that the initial magnitude of input current provided by C_0 would, in general, not coincide with a telemetry sampling point. However, the time at which the system switches to the calibration mode is essentially random with respect to the 32 samples per second telemetry data rate; consequently, observations of the calibration outputs in the neighborhood of T_0 over a period of a few minutes will enable one to select only those calibration sequences for which the peak signal observed is either a maximum or a minimum as compared to the peak signal values observed in all the other calibration sequences. The calibration sequences in which the peak output is a maximum are thus seen to correspond to the condition of a 1/32 second sample point having occurred just after the calibration relay circuit had

connected the output of C_0 to the input of the electrometer via R_0 . Alternatively, the calibration sequences in which the peak output is a minimum correspond to a 1/32 second sample point having occurred just before C_0 had been connected. The minimum peak signal would thus be smaller by a factor given by $e^{-\frac{\Delta T}{\tau}}$ where ΔT would be very nearly a whole sampling interval, i.e., 1/32 second. For a nominal time constant of .15 seconds this factor is given by

$$e^{-\left(\frac{1}{32} \times \frac{1}{.15}\right)} = .81$$

which indicates that errors of up to about 20% could be introduced if one ignores the effects of the data sampling characteristics when determining the time location of T_0 .

While the above procedure might tend to limit the use of the exponential portion of calibration to regions corresponding to the maximum and minimum peak values discussed above, it is not considered to be a severe restriction since no appreciable shift in system calibration would normally be expected to occur within time periods of a few minutes duration.

VI. TELEMETRY SYSTEM AND DATA FORMAT

The telemetry system was a PCM type utilizing two readout formats; one which sampled data each 30 msec (Format A) and a second which sampled each 15 msec (Format C). The analog data including signal and housekeeping information corresponding to the telemetered words are shown in Table 2 below. The number of words per frame was 120 for each of the formats (see Tables 3,4). Finally Table 5 charts the time interval between words important for situations where data variations may be occurring fast compared to sample times.

Measurement Description	No. Bits	Meas. No.	Response (SPS)	Telemetry Format	Range
PFA Density	8	K201	10	A,C	4×10^{-7} to 1×10^{-4} Amps
PFA Electronics Temp.	8	K202	0.1	A,C	
PFA Sensor High Voltage	8	K203	2	A,C	
PFA Baffle Status	8	K204	10	A,C	0 to 4 inches max.
CCG Range	8	K205	16	A,C	1×10^{-9} to 6×10^{-7} Amps
CCG Current	8	K206	16	A,C	4×10^{-7} to 1×10^{-4} Amps
CCG High Voltage	8	K207	1	A,C	
CCG Electronics Temp.	8	K208	0.06	A,C	
CCG Baffle Status	8	K209	10	A,C	0 to 4 inches max.
PFA Sensor Temp.	4	K221	0.1	A,C	
CCG Temperature	4	K222	0.06	A,C	
PFA Range	8	K211	10	A,C	1×10^{-9} to 6×10^{-7} Amps

DATA WORD DESIGNATION

TABLE 2

FORMAT A LAYOUT

BIT RATE=32K8PS FRAME LENGTH=128 WORDS

1	SYNC	SYNC	SYNC	MF 10	K150	K106	K260	10
11	K101		K140			K208		20
21	K231	K301	K302	K340	16 BIT SD	K206		30
	K232				SUB-FRAME			
31	K103		K140			K210		40
41	K104	M100 THRU M123		K150		K303		50
51	K105		K140			K211		60
61	K231	K301	K302	K340	K2	K2	K1	70
	K232				22	23	21	
71	K107		K140			M901		80
81	K209	16-BIT SD	K207	K150		K206		90
		SUB-FRAME						
91	K202		K140			K102		100
101	K203	K301	K302	K340	K205	K1	K2	110
					23	21		
111	K204		K140			K304		120

TABLE 3

FORMAT C LAYOUT

BIT RATE=64KUPS FRAME LENGTH=120 WORDS

```

.....
 1* SYNC* SYNC* SYNC*MF ID* K301* K302* K340* K101*K3*53* K204* 10
    *21*22*
.....
11* K211*      K260      *      *      * K303* K207* K140 20
    *      *      *      *      *      *      *
.....
21      K140      *      *      * K201* K123* H902* 30
    *      *      *      *      *      *      *
.....
31* K102*      K260      *      *      * K206*K1*K1* K304* 40
    *      *      *      *      *      *21*22*
.....
41* K106* 16-BIT SO * K202*      *      * K104*      K150 * 50
    *      * SUB-FRAME *      *      *      *      *
.....
51* K103*      K260      *      *      * K303* K205* K140 60
    *      *      *      *      *      *      *
.....
61      K140      *      *      * K201* 16-BIT SO * 70
    *      *      *      *      *      * SUB-FRAME *
.....
71* K211*      K260      *      *      * K206* K209* K304* 80
    *      *      *      *      *      *      *
.....
81* H100 THRU H123 * K203*      *      * H901* K231* K210* 90
    *      *      *      *      *      * *K232*
.....
91* K105*      K260      *      *      * K303* K208* K140 100
    *      *      *      *      *      *      *
.....
101      K140      *      *      * K201*      K150 *110
    *      *      *      *      *      *      *
.....
111* K107*      K260      *      *      * K206*K2*K2* K304*120
    *      *      *      *      *      *22*23*
.....

```

TABLE 4

FORMAT A

<u>Measurement Description</u>	<u>Measurement Number</u>	<u>Word</u>	<u>Word Time in Frame (Seconds)</u>	<u>Δt (Seconds)</u>
PFA Density	201	67	.01675	---
PFA Range	211	57	.01425	---
CCG Range	205	105	.02625	---
CCG Current	206	27	.00675	---
CCG Current	206	87	.02175	.0150

Frame rate is .030 seconds, time between words is .000250 seconds

FORMAT C

<u>Measurement Description</u>	<u>Measurement Number</u>	<u>Word</u>	<u>Word Time in Frame (Seconds)</u>	<u>Δt (Seconds)</u>
PFA Density	201	28	.00350	---
PFA Density	201	68	.00850	.0050
PFA Density	201	108	.01350	.0050
PFA Range	211	11	.001375	---
PFA Range	211	71	.008875	.0075
CCG Range	205	49	.006125	---
CCG Current	206	38	.00475	---
CCG Current	206	78	.00975	.0050
CCG Current	206	118	.01475	.0050

Frame rate is .015 seconds, time between words is .000125 seconds

Table B Telemetry Timing Format

VII. FLIGHT RESULTS

In March of 1978 the S3-4 payload carrying the CRL-737 experiment was launched into an elliptical orbit with a perigee near 165 KM and apogee of ~270 KM. The mean atmospheric density ratio at these altitudes is approximately 20 to 1 with higher or lower ratios possible depending on solar-geophysical circumstances.

The breakoff mechanisms of the two instruments exposing the inlet tubulations to the atmosphere were actuated successfully during the first orbit. System power to the gauges was not applied until orbit 99 on March 22, at which time a series of nine PFA baffle deployments were ground commanded beginning at 2129 GMT and ending at 2154 GMT. These are shown in the microfilm printout in Figure 18. Examination of the data indicates that the baffle functioned properly with the extension mechanism working normally. Also the in-flight calibration occurring at 2030 GMT for the PFA and approximately a minute earlier for the CCG is in accord with the pre-launch calibration. The step current at 1×10^{-6} Amp indicates the proper PFA TM voltage of 1.75V on the Low Gain Channel (K211). Corresponding CCG voltages of 1.36V and 4.9V on K206 and K205 were also in agreement with the pre-launch calibration.

In the months following the satellite launching several types of flight records were made available to us by the Air Force Geophysics Laboratory. These included computer printouts (primarily in Format A) in which listings in each of the data outputs from the CCG and PFA were separately tabulated. Also available were selected complete orbits in which the TM data had been processed to yield atmospheric density in a manner for direct comparison with the model atmosphere. A third type of data represented analog plots of current output for each of the instruments in which both the high gain and low gain channels could be compared.

The analysis encompassed a variety of tasks including a detailed examination of the internal electronic calibration. Baffle deployment was examined to ensure that the baffle commands resulted in an appropriate response. For example, many orbits were examined to determine whether or not the baffle on either instrument was impeded in either extending or retracting. Of particular interest was an examination of the modulation depth or extinction of the gauge current as a function of extension.

a) In-Flight Electronic Calibration

Our first emphasis in examining the data was to establish that the in-flight calibration had not deviated from the laboratory calibration. To this end we have examined many orbits beginning with Orbit 99 occurring on March 22, 1978 through late orbits such as 2470 occurring on August 15, 1978.

In our check of the calibration data we have considered the fact that the PCM word corresponding to the high and low gain outputs (i.e., Range

and Density) are sampled at differing times. The word separation for the PFA instrument is K211 (word 57) and K201 (word 67) or a lapsed time of 2.5 milliseconds. This corresponds to an error of approximately 2% based on a decay constant $\tau = .160$ sec. for the PFA. Correspondingly the word separation for the CCG using the K205 (word 105) and K206 (word 87) or a time difference of 4.5 milliseconds or an error of 3%. The choice K206 (word 27) referenced to K205 (word 105) would have represented a substantial larger error (approaching 10%) based on a decay constant $\tau = .155$ sec.

As may be seen in Figures 19 and 20 the CCG appears to have maintained its calibration, virtually unchanged, from the beginning of the flight to the end. Similarly, the PFA instrument over most of its entire dynamic range is observed to have held calibration. At the low current end of both the high and low gain channels, however, is noted a deviation from true logarithmic. This non-linearity appears even for some early orbits for example, Orbit 99 as may be seen in Figure 20. Such an effect would result in erroneous currents for the PFA particularly at the low end of the instrument (less than 2×10^{-7} A) and would have the effect of bringing the CCG and PFA into somewhat better agreement if a correction were made at the higher altitudes. It would not however influence the differences observed in the two instruments at the higher currents observed at lower altitudes.

With respect to the data itself, both instruments experienced an effect not seen in the auto-calibrations. Examination of Figures 21, 22 illustrate an anomalous situation between the high and low gain outputs of each instrument (somewhat more severe in the CCG). While the calibration current on both the high and low gain channels track well over the entire domain of the current overlap region (Refer to Fig. 15, 16) the current from cathode gauge do not track for the two outputs. This is true both in the actual atmospheric density measuring mode and also during all baffle deployments. The series Figures 21 through 26 illustrate that the anomalous behavior lasted throughout the flight and remained constant. Figures 25 and 26 illustrate that the effect existed over the entire overlap region for the CCG ($2 \times 10^{-7} - 10^{-6}$ Amp) while for the PFA the effect begins for currents less than 3×10^{-7} Amps. These figures demonstrate the uniformity of the effect for both ambient currents and baffle situations.

b) High Voltage and Temperature Monitors

Our examination of the high voltage history of both Cabot gauges over the satellite lifetime indicates that there was no significant variation. The listing of the high voltage outputs from the telemetry and converted to the gauge anode high voltage is illustrated in Table 6.

As mentioned in the introduction the gauge sensitivity is approximately 0.5 amperes per Torr per 450 volts or approximately 1 ma/per Torr per volt. From Table 6 the variation of approximately +25 volts in the CCG

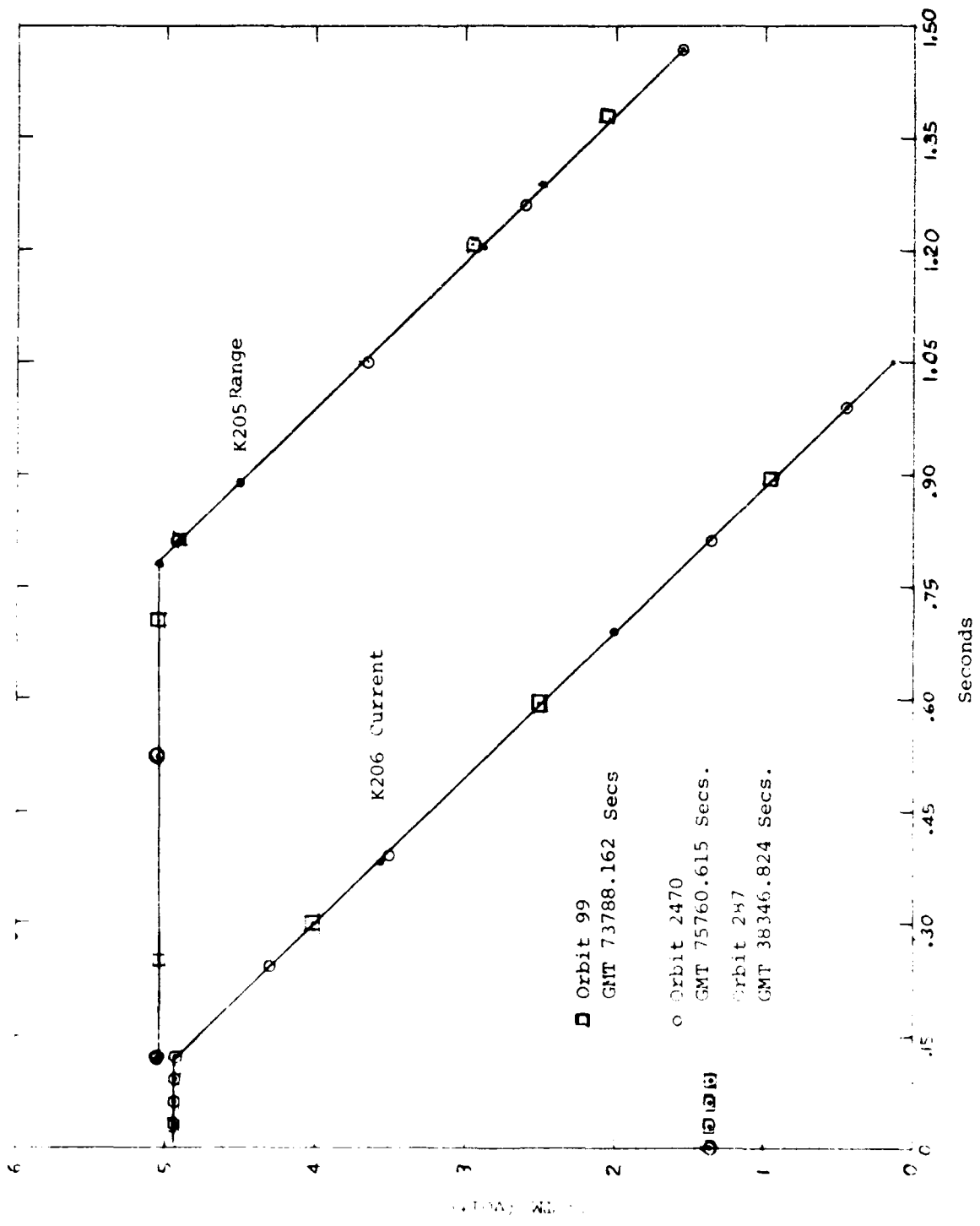


Figure 19 CCG In-Flight Calibration

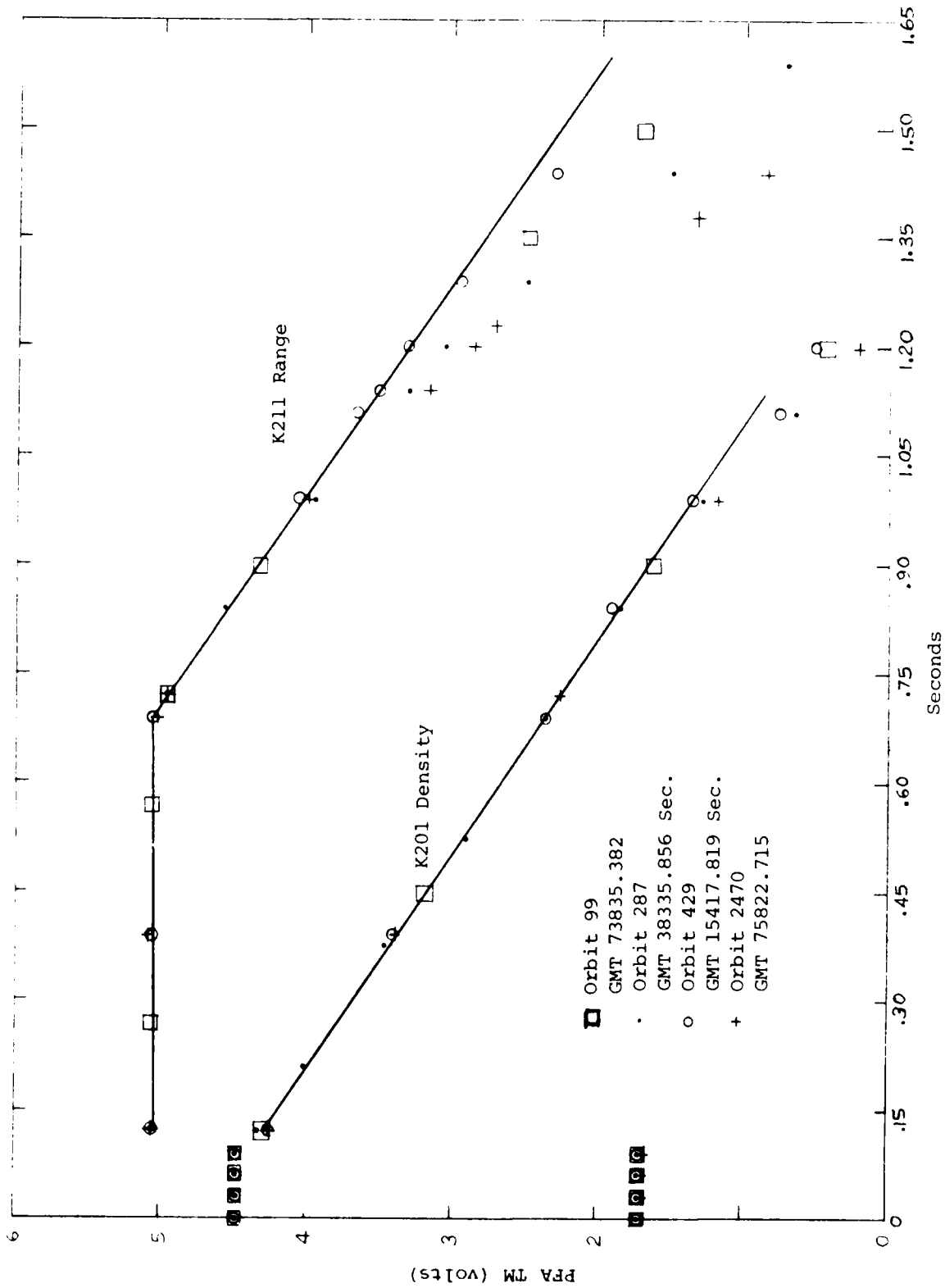


Figure 20 PFA In-Flight Calibration

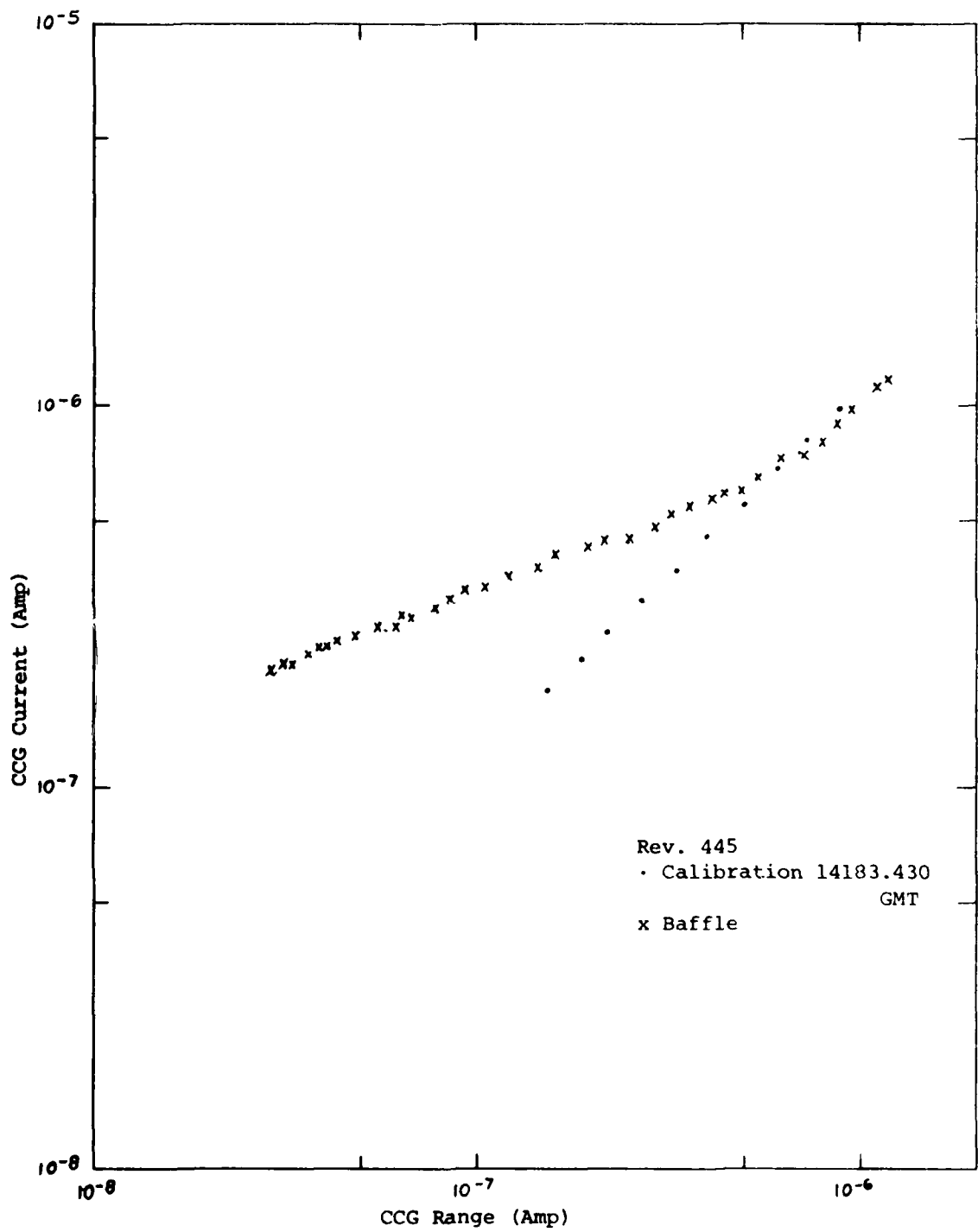


Figure 21 CCG Dual Range Comparison
(from computer printout)

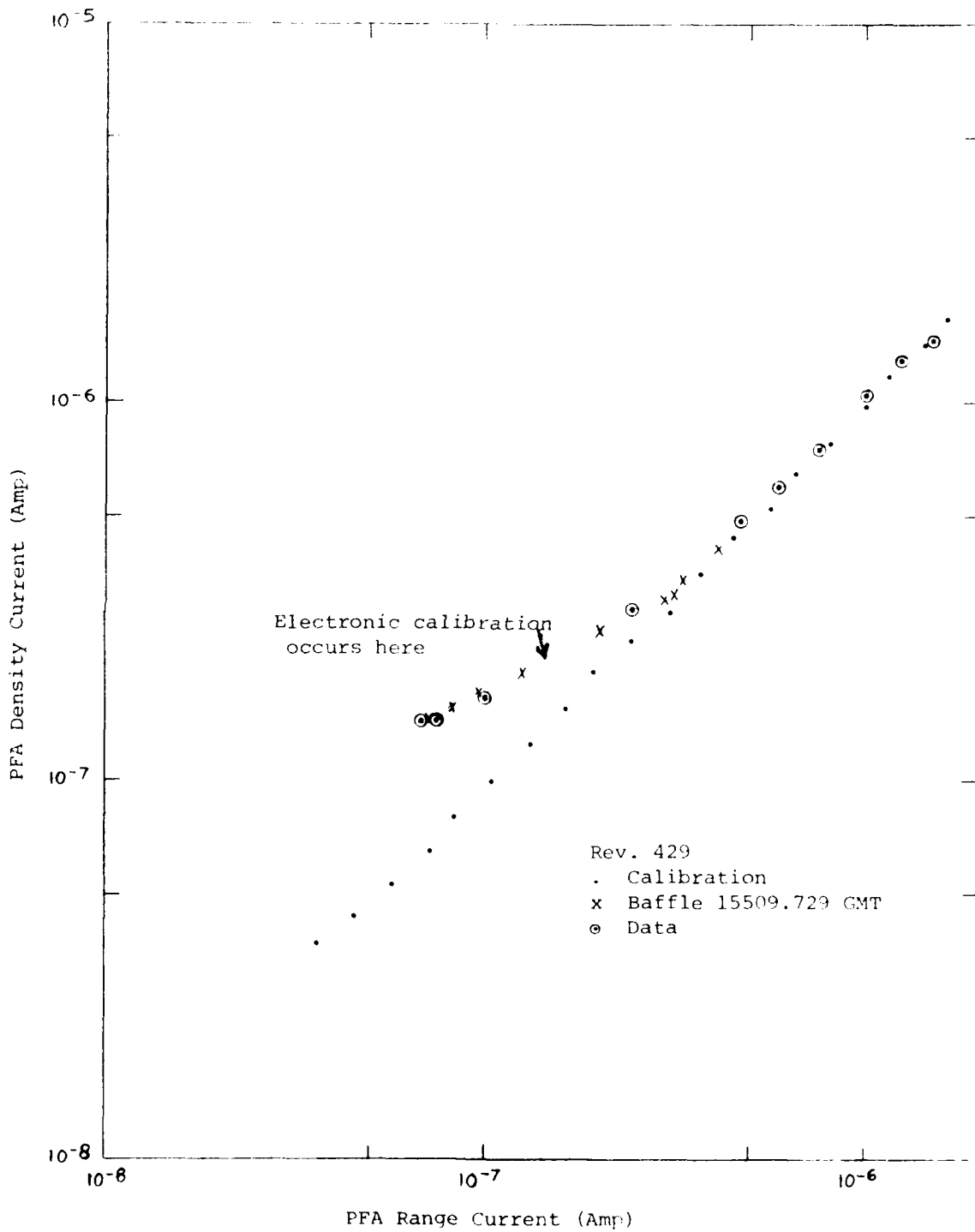


Figure 22 PFA Dual channel comparison
(from computer printout)

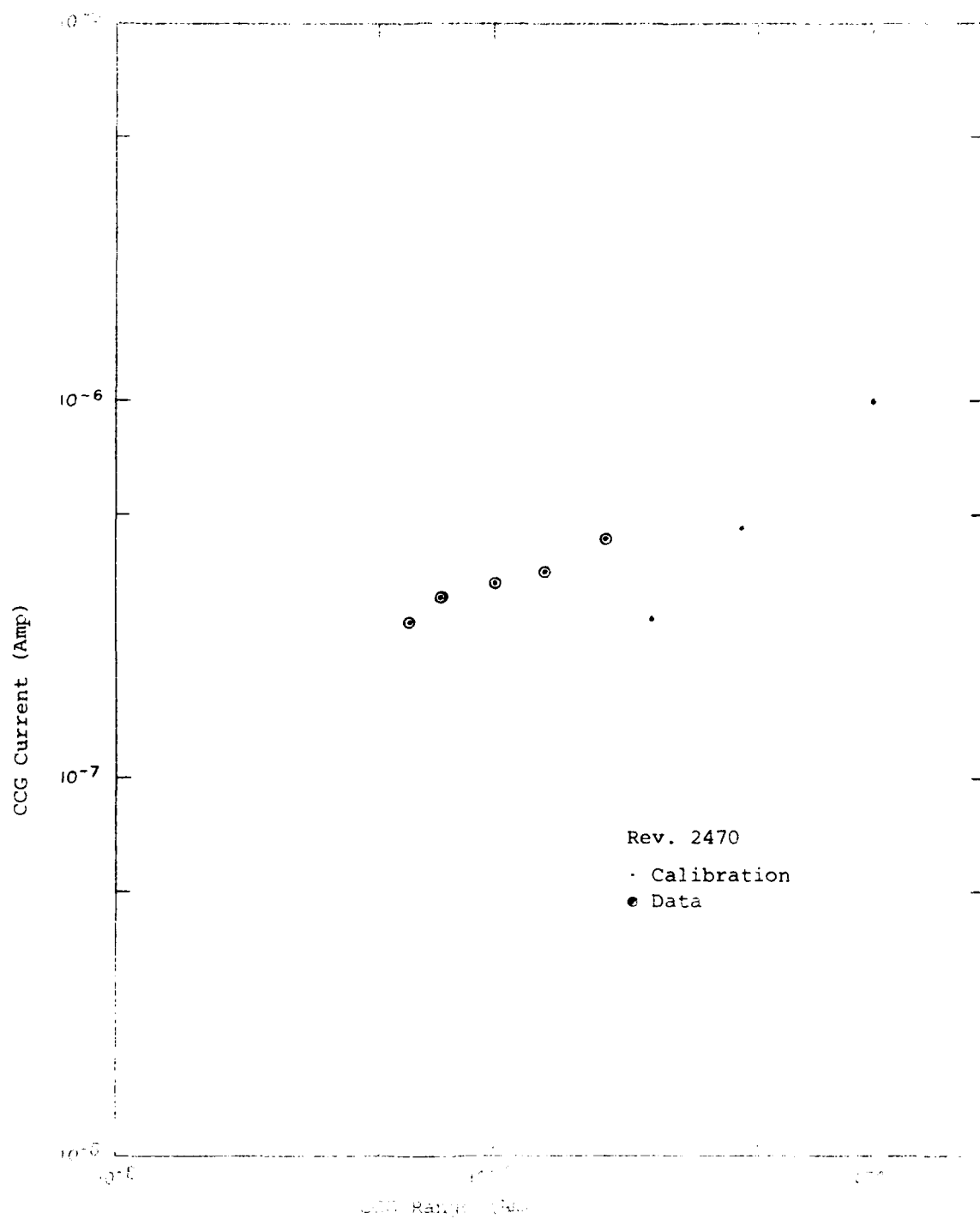


Figure 10. Dual Channel, precision
 range comparison plot.

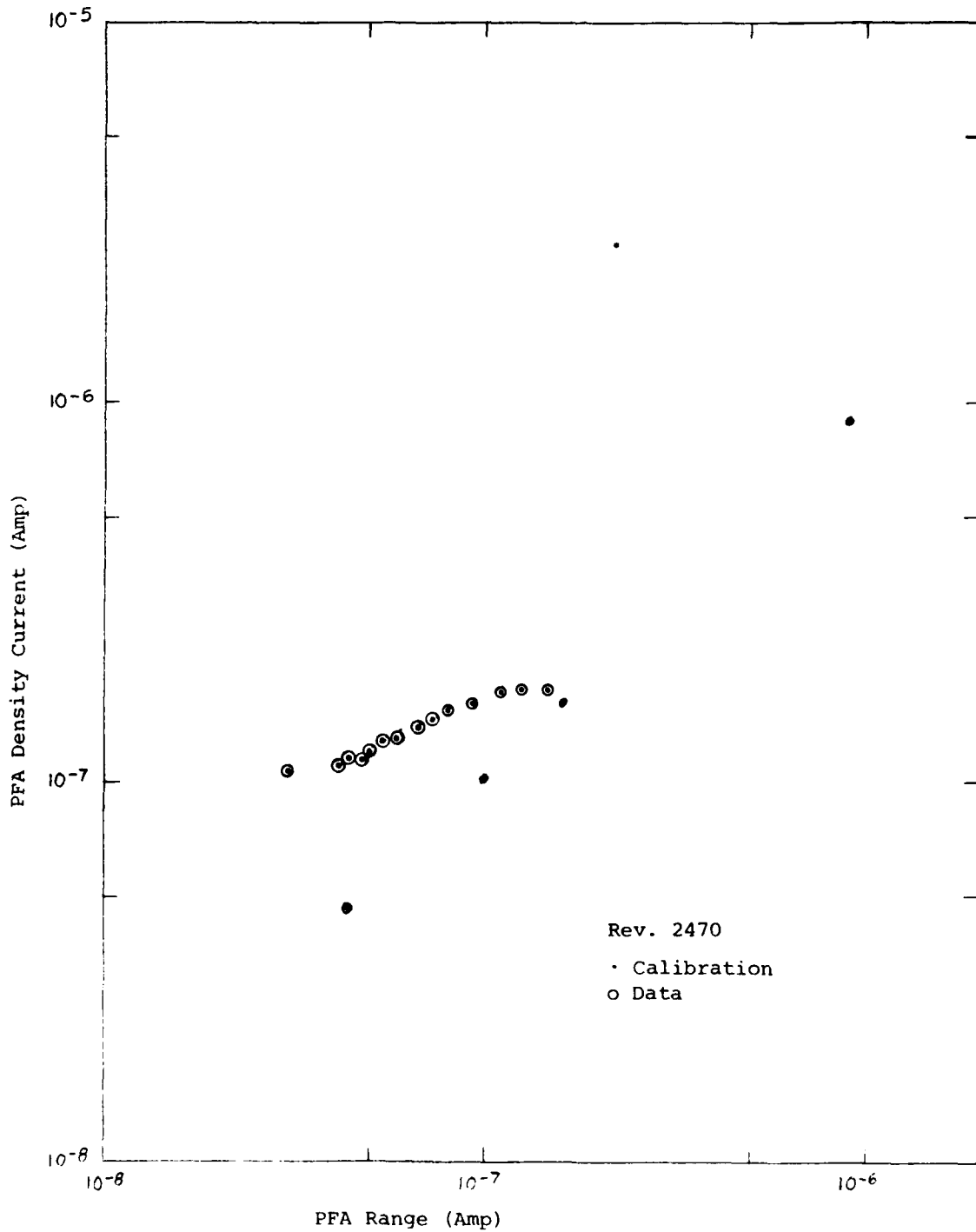


Figure 24 PFA Dual Channel Comparison
(from computer printout)

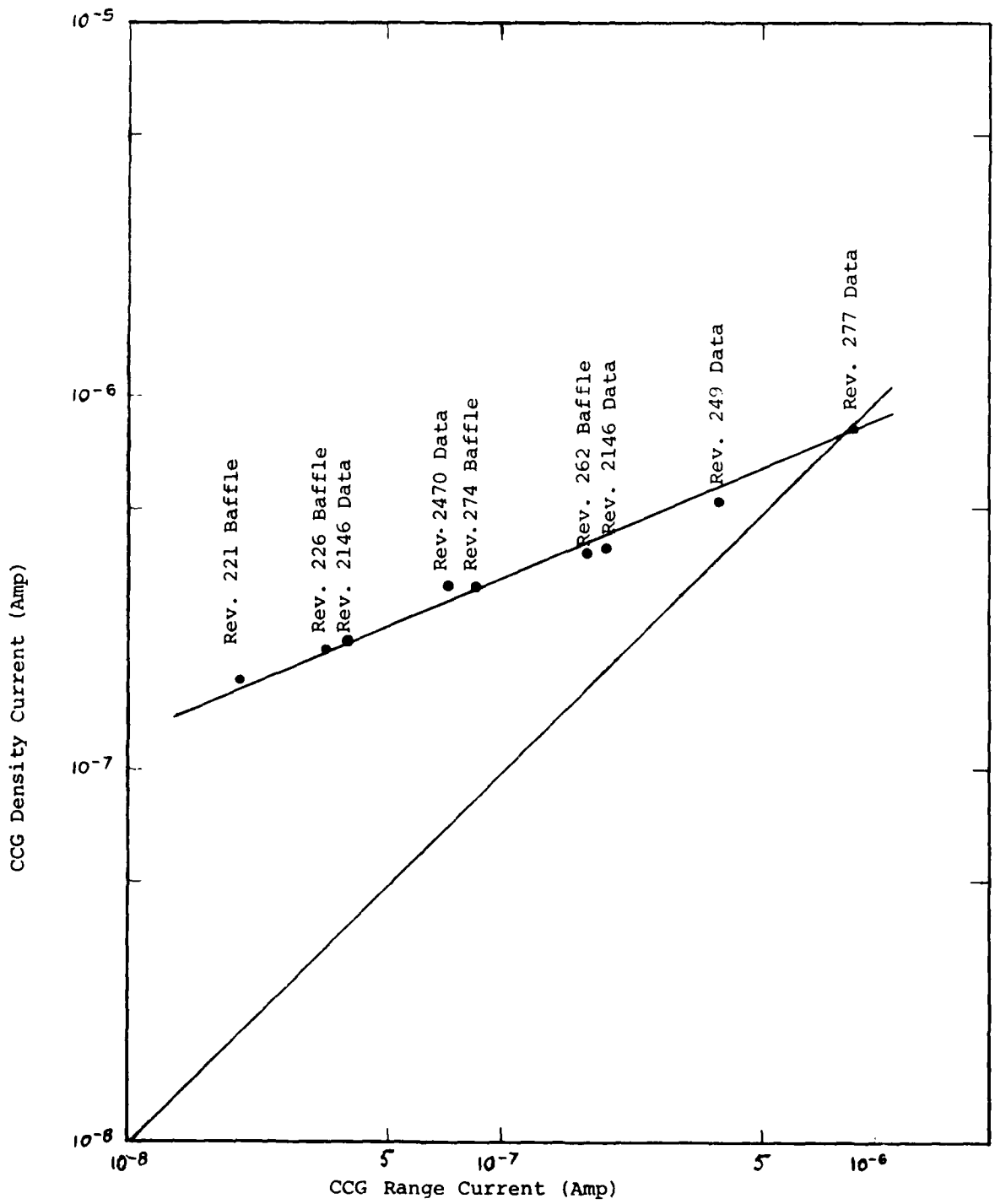


Figure 25 CCG Dual Channel Comparison
(Data obtained from microfilm)

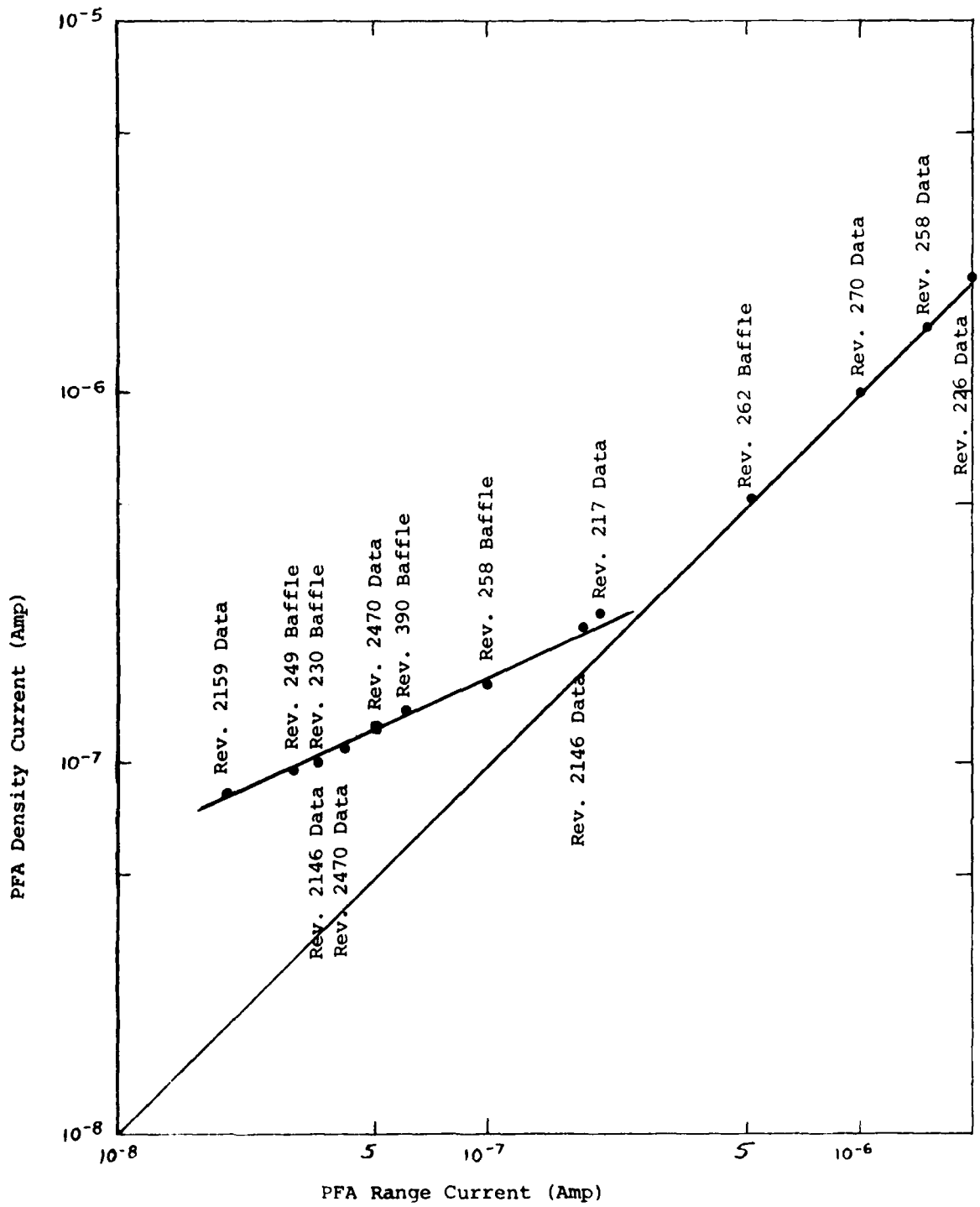


Figure 26 PFA Dual Channel Comparison
(Data obtained from microfilm)

COLD CATHODE GAUGE HIGH VOLTAGE HISTORY

<u>ORBIT</u>	<u>DATE</u>	<u>H. V. Monitor (VOLTS)</u>	<u>High Voltage (VOLTS)</u>
99	3/22/78	CCG 3.58 - 3.60 PFA 3.72 - 3.74	1816 - 1826 1770 - 1778
164	3/26/78	CCG 3.60 - 3.62	1820 - 1825
287	4/3/78	CCG 3.56 - 3.58 PFA 3.70 - 3.74	1816 - 1826 1770 - 1778
291	4/3/78	CCG 3.56 - 3.58 PFA 3.68 - 3.76	1816 - 1826 1752 - 1780
377	4/9/78	CCG 3.56 - 3.58 PFA 3.70 - 3.76	1816 - 1826 1770 - 1780
429	4/12/78	CCG 3.58 - 3.60 PFA 3.72 - 3.76	1816 - 1826 1770 - 1780
439	4/12/78	CCG 3.58 PFA 3.74 - 3.76	1826 1778 - 1780
445	4/13/78	CCG 3.56 - 3.58 PFA 3.74 - 3.76	1816 - 1826 1778 - 1780
2470	8/15/78	CCG 3.64 - 3.66 PFA 3.78 - 3.84	1844 - 1853 1795 - 1812

TABLE 6

gauge and -30 volts in the PFA gauge would result in pressure errors of approximately +2% and -3% respectively.

Table 7 provides a quick look of the temperature history of the instruments including the gauges and electronics boxes. It is seen that the coldest temperature occurred in the early orbits; this has been attributed to the fact that equipment power was not applied until Orbit 99 at which time temperatures between -9°C and -15°C are recorded. A general warming up and stabilizing of the temperature occurs after several hundred orbits. No temperature excursion of significance are observed with the measured temperatures well within the required operating limits of -20°C to $+70^{\circ}\text{C}$.

c) Baffle Performance

A review of the baffle performance over many orbits indicates that this mechanical function operated very reliably and in all instances full extension occurs at 10.07 cm for the CCG and 9.37 cm for the PFA instruments. Deployment times (extension and retraction) are 63 seconds and 56 for the respective instruments. Some variability in the overall time is observed primarily due to the fact that the incremental motor advancing the brass foil returns to a discrete home base position which varies from one deployment to the next. Table 8 illustrates some sample TM voltages for the PFA position and the CCG position representing the fully retracted baffle for various orbits.

ORBIT	PFA	K204	CCG	K209
99	.24V	.062"	.18V	.07"
164	-	-	.34V	.19"
287	.18/.20V	0"	.18V	.07"
291	.32V	.13"	.18V	.07"
377	.14V	0"	.18V	.07"
429	.18V	0"	.18V	.07"
439	.32V	.13"	.32V	.19"
445	.18/.32V	.13"	.18V	.07"
2470	.22V	.06"	.18V	.07"

TABLE 8 FULLY RETRACTED BAFFLE POSITION

The linearity of the extension with time has been checked for many orbits and Fig. 27, 28 are representative. The deployment rates are .30 cm/sec and .33 cm/sec for the CCG and PFA baffles respectively.

As mentioned earlier the baffle extension serves to provide aspect angle data by analyzing the obscuration of the gas flow to the gauge as a function of baffle position. One technique employed by J. McIsaac at the Air Force Geophysics Laboratories identifies the instant at which the gauge current indicates that atmospheric flow has been impeded. The angle whose tangent arms are the baffle length at the time referred to above (measured from the break-off point) and the lateral distance from the

REV. NO.	DATE	PFA		CCG	
		K202	K211	K208	K222
		ELECT. TEMP.	GAUGE TEMP.	ELECT. TEMP.	GAUGE TEMP.
99	3/22/78	1.62V - 1.64V -9°C		1.60V - 1.64V -11°C	1.42V -15°C
164	3/25/78	no record		1.78V - 1.84V -5°C - 6°C	1.74V -7°C
287	4/03/78	1.82V - 1.92V -3°C - -1°C	1.74V -7°C	1.82V - 1.96V -6°C - -2°C	1.74V -7°C
291	4/03/78	1.96V - 2.02V +2°C	2.06V - 1.74V 1°C - -7°C	1.86V - 2.02V 0°C	1.74V -7°C
377	4/09/78	1.92V - 2.04V 0°C - 2.5°C	2.06V 1°C	1.90V - 2.04V -3°C - -1°C	1.74V - 2.06V -7°C - -1°C
429	4/12/78	2.04V - 2.08V 2.5°C - 4°C	2.06V 1°C	2.06V - 2.10V 2°C	2.06V 1°C
439	4/12/78	2.10V - 2.14V 4°C - 6°C	2.06V 1°C	2.10V - 2.16V 2°C - 4°C	2.06V 1°C
445	4/13/78	2.08V - 2.16V 6°C	2.06V 1°C	2.10V - 2.18V 2°C - 5°C	2.06V 1°C
2470	8/15/78	2.08V - 2.20V 4°C - 7°C	2.06V 1°C	2.06V - 2.24V 1°C - 6°C	2.06V 1°C

TABLE 7 TEMPERATURE DATA HISTORY

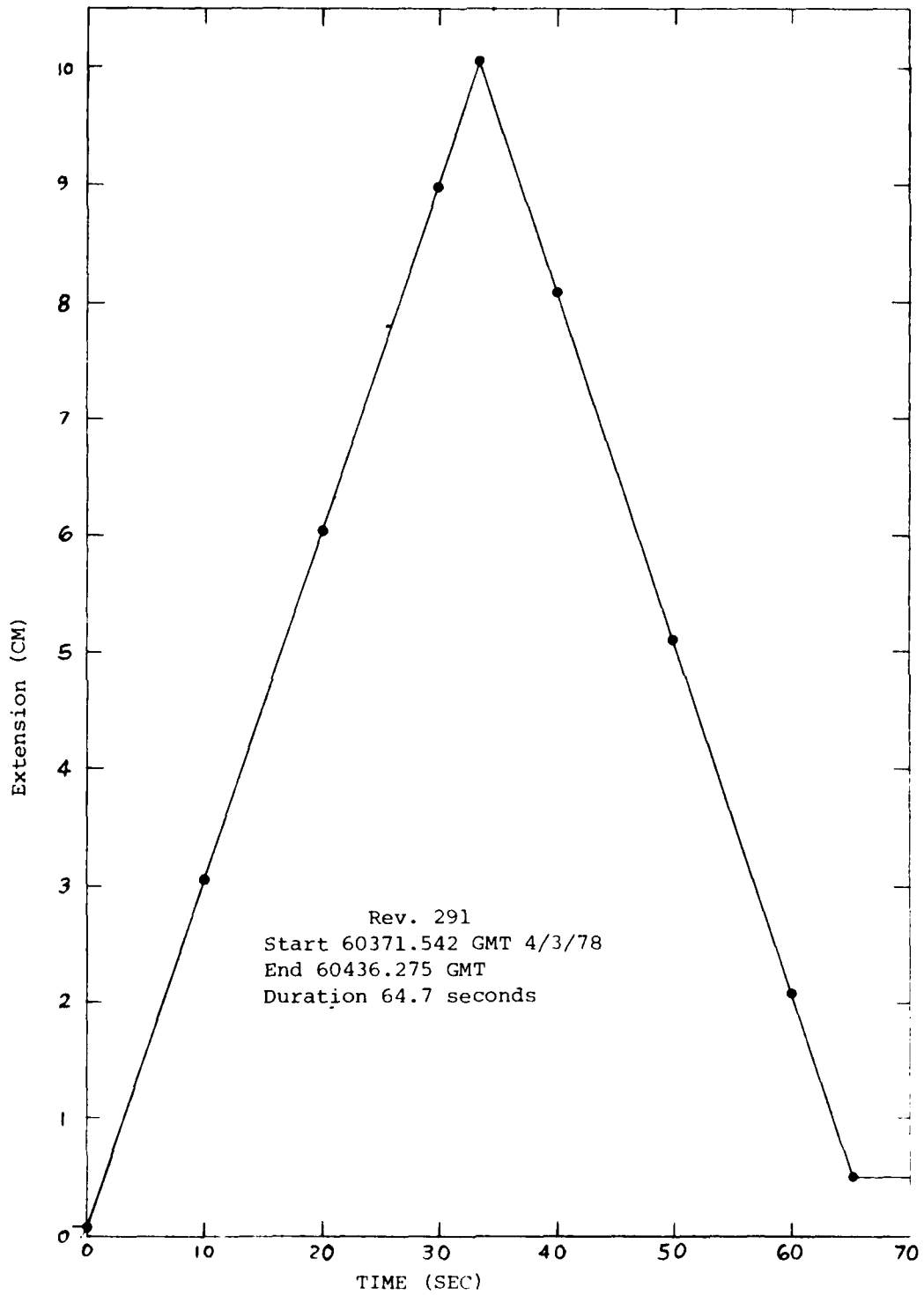


Figure 27 CCG Baffle Deployment

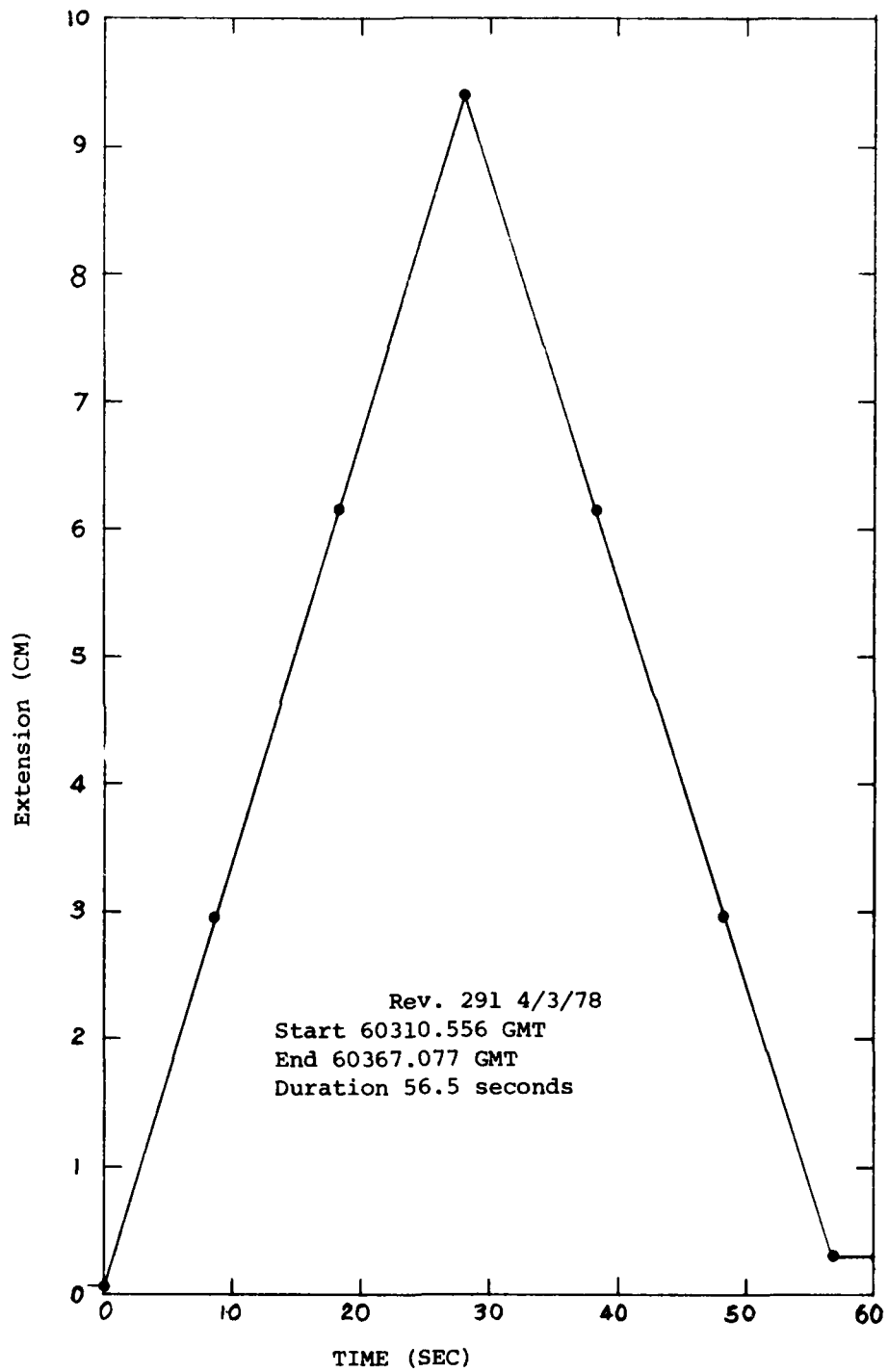


Figure 28 PFA Baffle Deployment

baffle to the edge of the entrance orifice defines the angle of attack. This technique has been used successfully in the present flight and corroborates the 45° mounting of the gauge to the satellite velocity vector over the perigee region particularly.

Perhaps the most anomalous behavior of the baffle mechanism is associated with the depth of modulation observed in the two instruments. Figures 29-32 serve to illustrate the effect. A comparison of baffle deployments at approximately the same time for the CCG and PFA reveals the following. Comparing both low gain and high gain outputs of the two instruments at maximum baffle extension indicates that the CCG current interruption is much larger. In particular, at lower altitudes the effect appears more pronounced. For example, in the case of Orbit 221 comparing the low gain outputs at an altitude of 223 KM the current attenuation at maximum baffle deployment for the CCG is greater than 6 times more influential than for the PFA (Figures 29,30). At lower altitudes nearer perigee the effect is somewhat less pronounced; however, Figures 31,32 indicate that the CCG experiences a 5 times greater attenuation than the PFA at maximum deployment for an altitude corresponding to 168 - 170 KM. Table 9 provides the extent to which this phenomenon was observed over a sample of many orbits. In general the PFA instrument seems to lag the CCG suggesting a possible time constant effect or lesser gauge conductance.

The argument for a reduced conductance in the PFA gauge which as mentioned earlier did not possess a perforated cathode may receive additional support from Figures 33,34. These represent a linear plot of current extinction for two baffle deployments occurring within a minute of each other on Orbit 429 at an altitude of 251 KM. It will be noticed that the current response to baffle extension is substantially faster in the CCG case. The rate of current change for the CCG is measured as 1.37×10^{-7} Amps/Sec and $.36 \times 10^{-7}$ Amps/Sec for the PFA for approximately the same baffle deployment rates. The factor of 3.8 difference implies that perhaps the extinction of current is not reached in the PFA. Reviewing the baffle deployments over many of the microfiche records further supports the view that the PFA responds slower to baffle action than the CCG.

During later orbits the baffle deployments evidences a strange current behavior in both instruments as is seen in Figures 35,36. The double peaked troughs suggest the possibility of a satellite attitude change during the deployment period. That the orientation of the gauge to the flow is changing is corroborated by the fact that at the time of maximum baffle extension the current exceeds the ambient levels by a substantial amount particularly in the CCG. Here again the response time for the CCG is seen to be much faster. The spin period reflected in the modulated output is approximately 30 seconds.

It is important to mention, however, that the notion that the PFA gauge, in particular, and possibly the CCG to a lesser extent suffered from lower than anticipated conductances is not totally unexpected. For example, a similar gauge was fabricated by F. Torney, Cabot Corporation for use

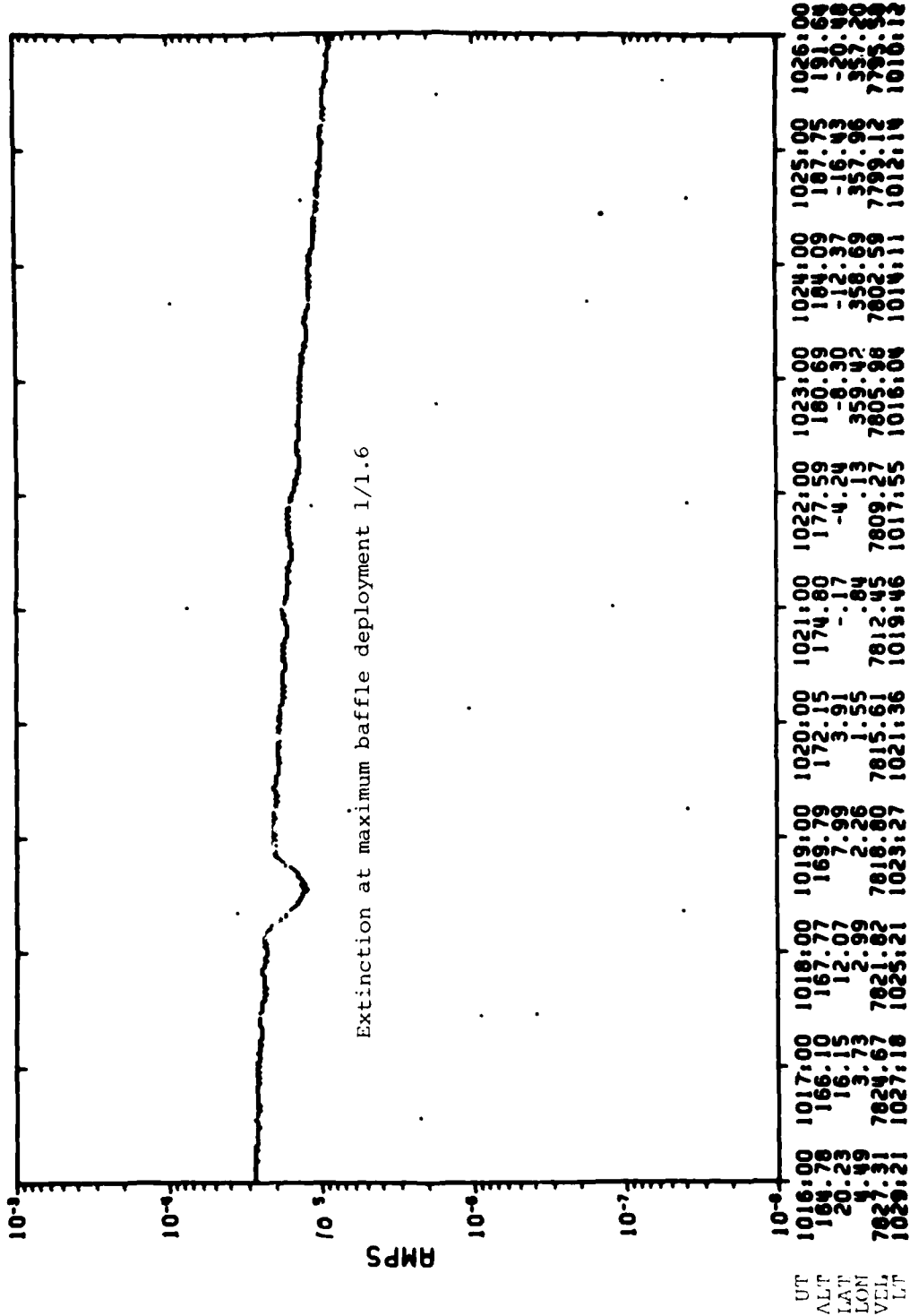


Figure 29 Sample Orbit illustrating baffle deployment

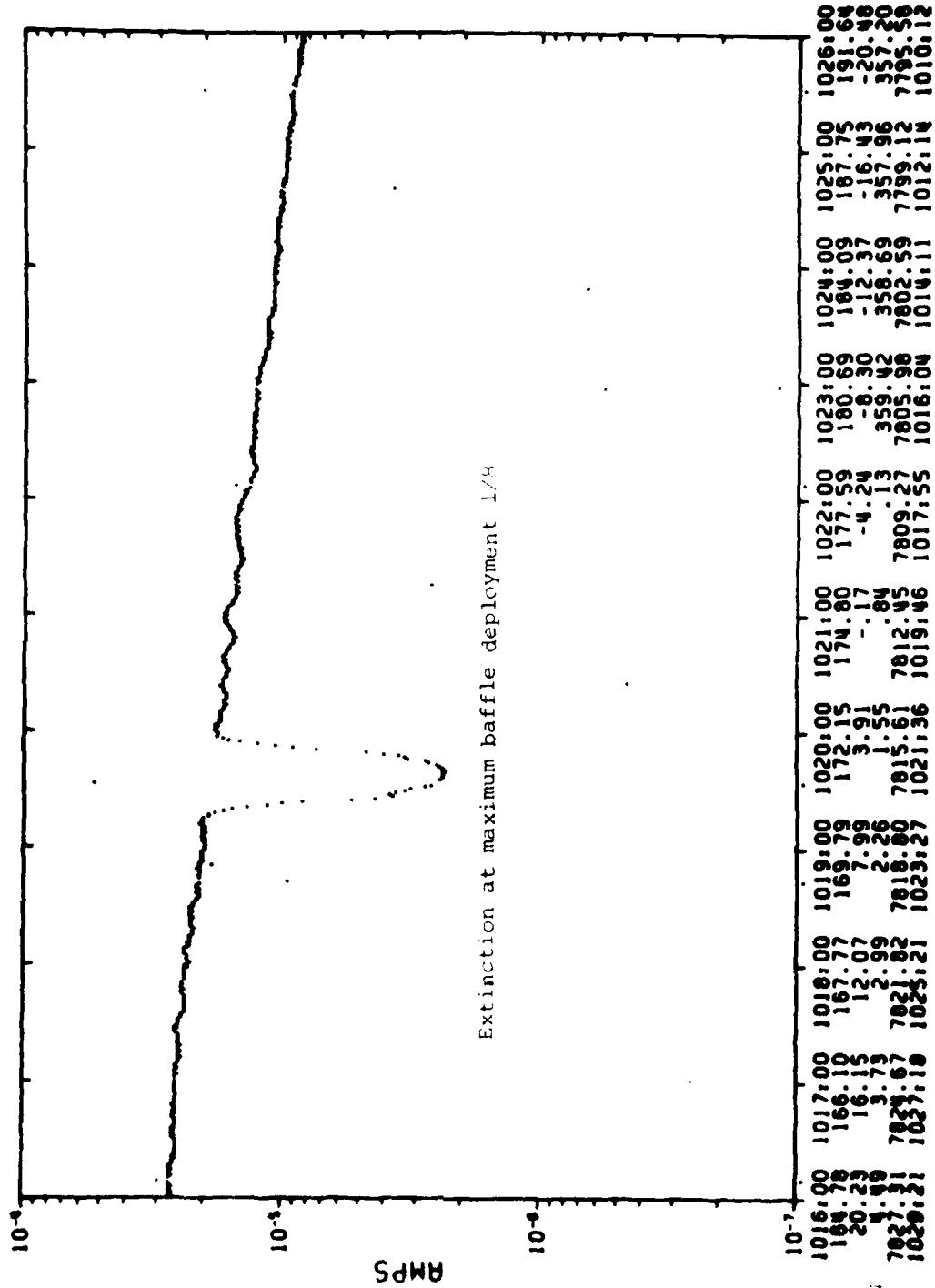


Figure 30 Sample Orbit illustrating baffle deployment

CAL-737 PFA RANGE REV 0221 03/30/78

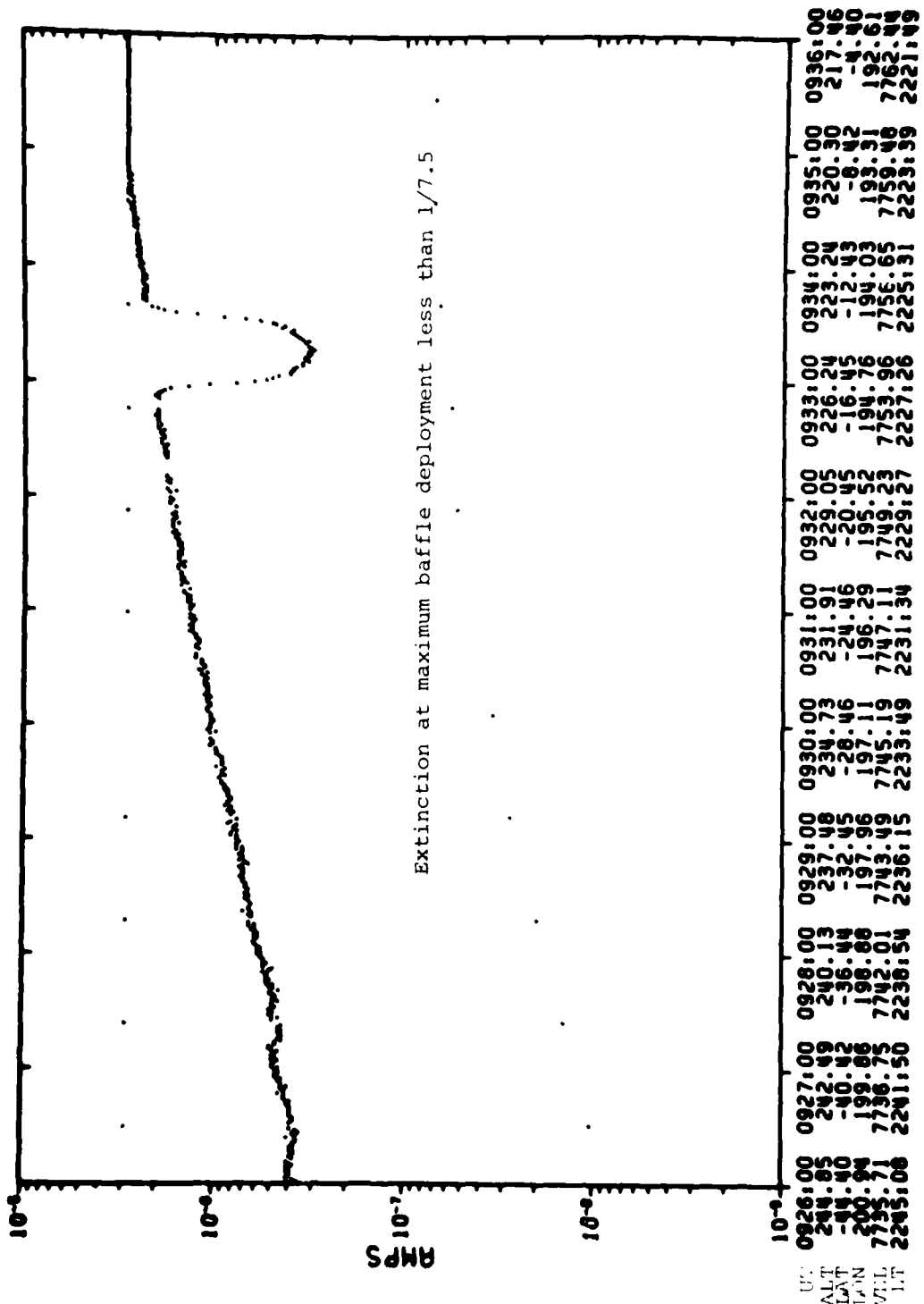
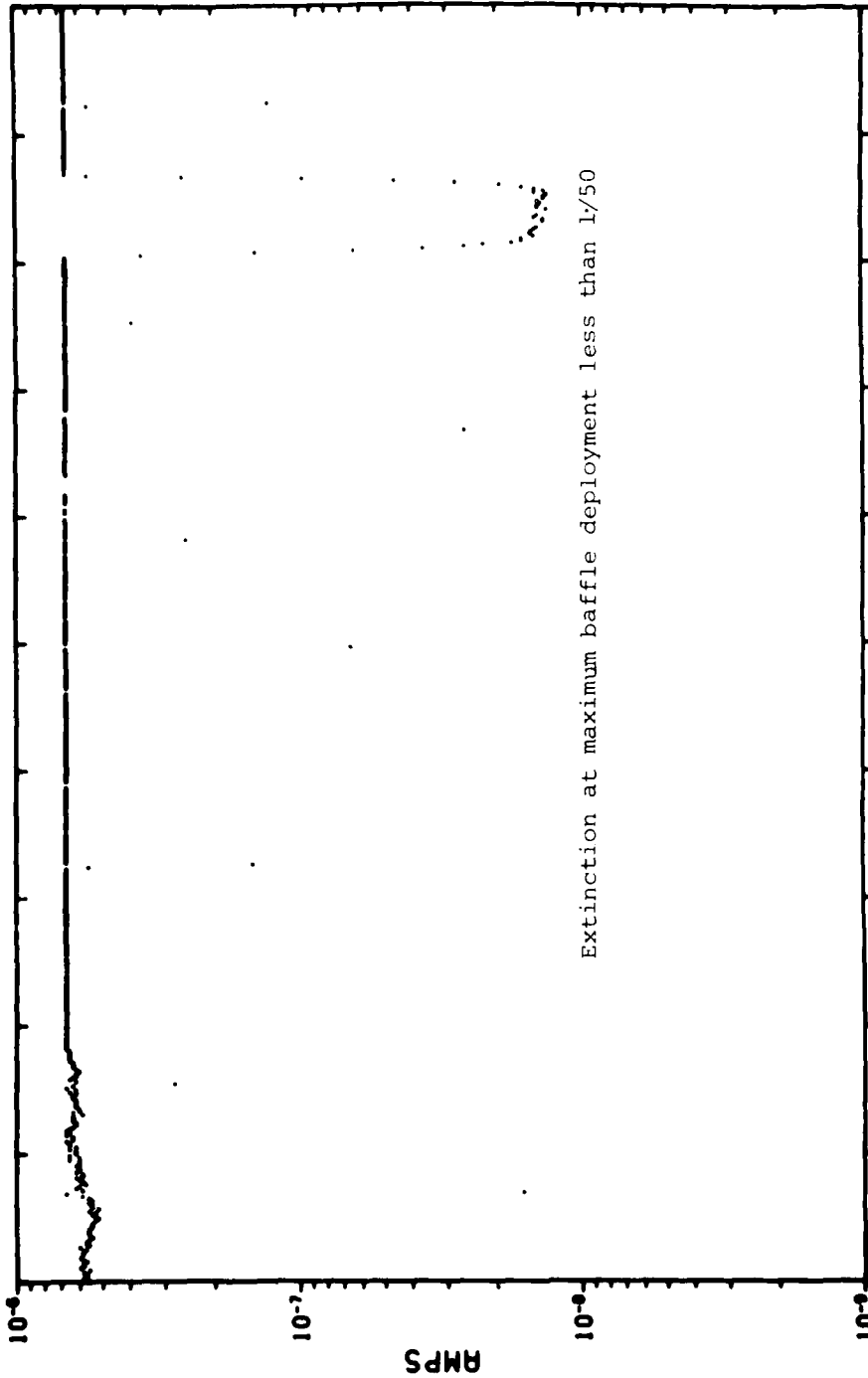


Figure 31 Sample Orbit illustrating baffle deployment



Extinction at maximum baffle deployment less than 1/50

UT	ALT	LAT	LOH	VEL	LT
0926:00	244.85	-44.40	200.94	7735.71	2245:08
0927:00	242.49	-40.42	199.86	7736.75	2241:50
0928:00	240.13	-36.44	198.88	7742.01	2238:54
0929:00	237.48	-32.45	197.96	7743.49	2236:15
0930:00	234.73	-28.46	197.11	7745.19	2233:49
0931:00	231.91	-24.46	196.29	7747.11	2231:34
0932:00	229.05	-20.45	195.52	7749.23	2229:27
0933:00	226.24	-16.45	194.76	7753.96	2227:26
0934:00	223.24	-12.43	194.03	7756.65	2225:31
0935:00	220.30	-8.42	193.31	7759.48	2223:39
0936:00	217.46	-4.40	192.61	7762.44	2221:49

Figure 32 Sample Orbit illustrating baffle deployment

<u>ORBIT</u>	<u>DATE</u>	<u>ALTITUDE</u>	<u>PFA RANGE</u>	<u>PFA DENSITY</u>	<u>CCG RANGE</u>	<u>CCG CURRENT</u>
217 KM	3/30/78	165 KM	Saturation	1/1.8	Saturation	1/9
		252 KM	1/4	1/2	1/55	No data
221 KM	3/30/78	168 KM	Saturation	1/1.6	Saturation	1/8
		225 KM	1/7	1/5	1/50	1/20
226 KM	3/30/78	169 KM	Saturation	1/1.6	Saturation	1/8
		214 KM	1/5.5	1/4	<1/30	1/20
244 KM	3/31/78	167 KM	Saturation	1/1.6	Saturation	1/8
		228 KM	1/9	1/4.5	<1/70	1/15
249 KM	4/1/78	155 KM	Saturation	1/2	Saturation	1/9
		259 KM	1/3	1/2	1/30	Off scale
301 KM	4/4/78	163 KM	Saturation	1/1.6	Saturation	1/6
		259 KM	1/4.5	1/2	1/90	Off scale
382 KM	4/9/78	205 KM	< 1/1.4	1/2	<1/7	1/25
		255 KM	1/7	1/2	1/60	Off scale
425 KM	4/11/78	202 KM	Saturation	1/1.8	<1/3	1/20
		255 KM	1/6	1/2	1/70	Off scale
445 KM	4/13/78	200 KM	Saturation	1/1.5	<1/8	1/60
		243 KM	1/4	1/2.2	1/70	Off scale

TABLE 9 DEPTH OF MODULATION (current attenuation at maximum baffle extension)

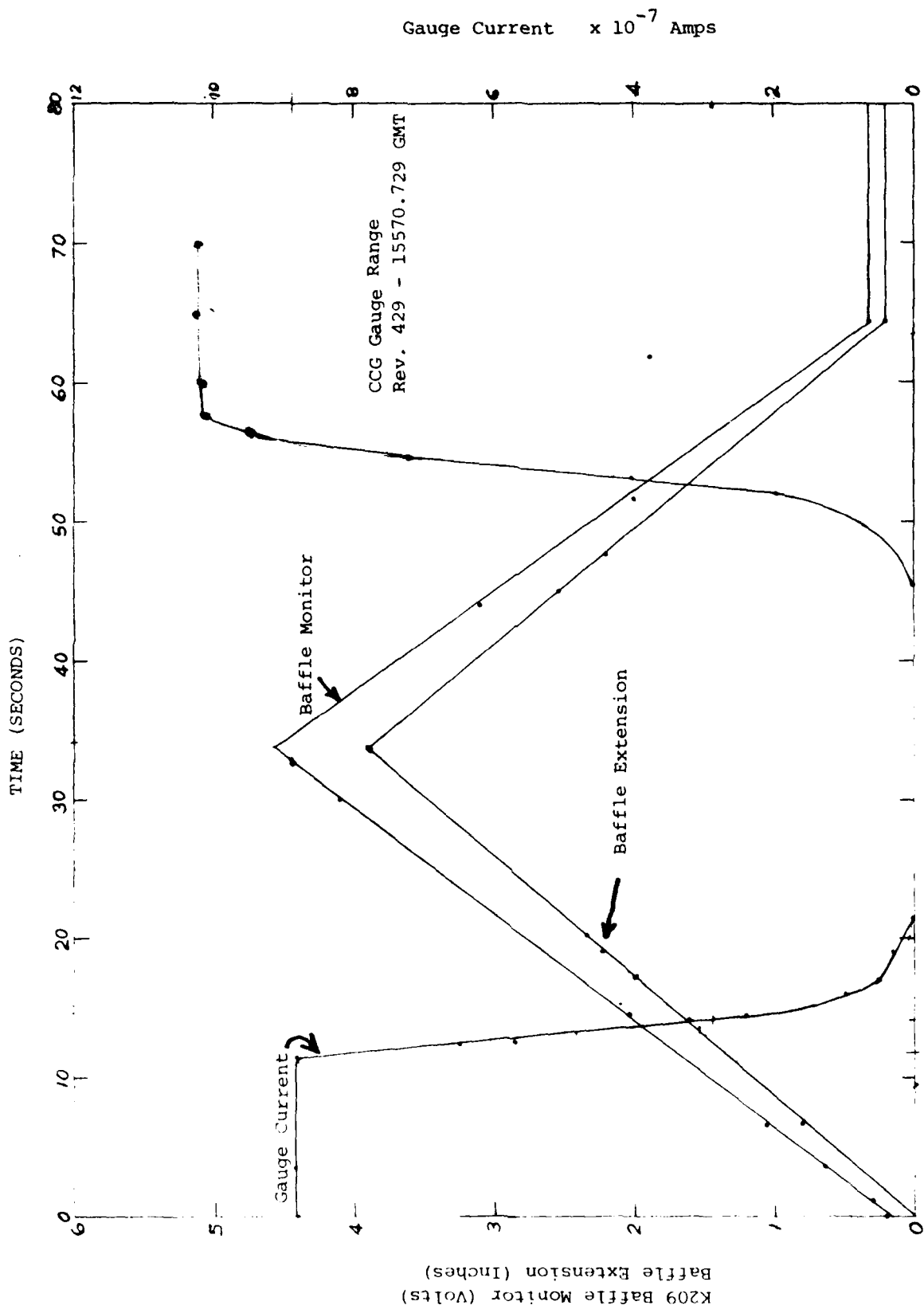


Figure 33 Sample Baffle Deployment

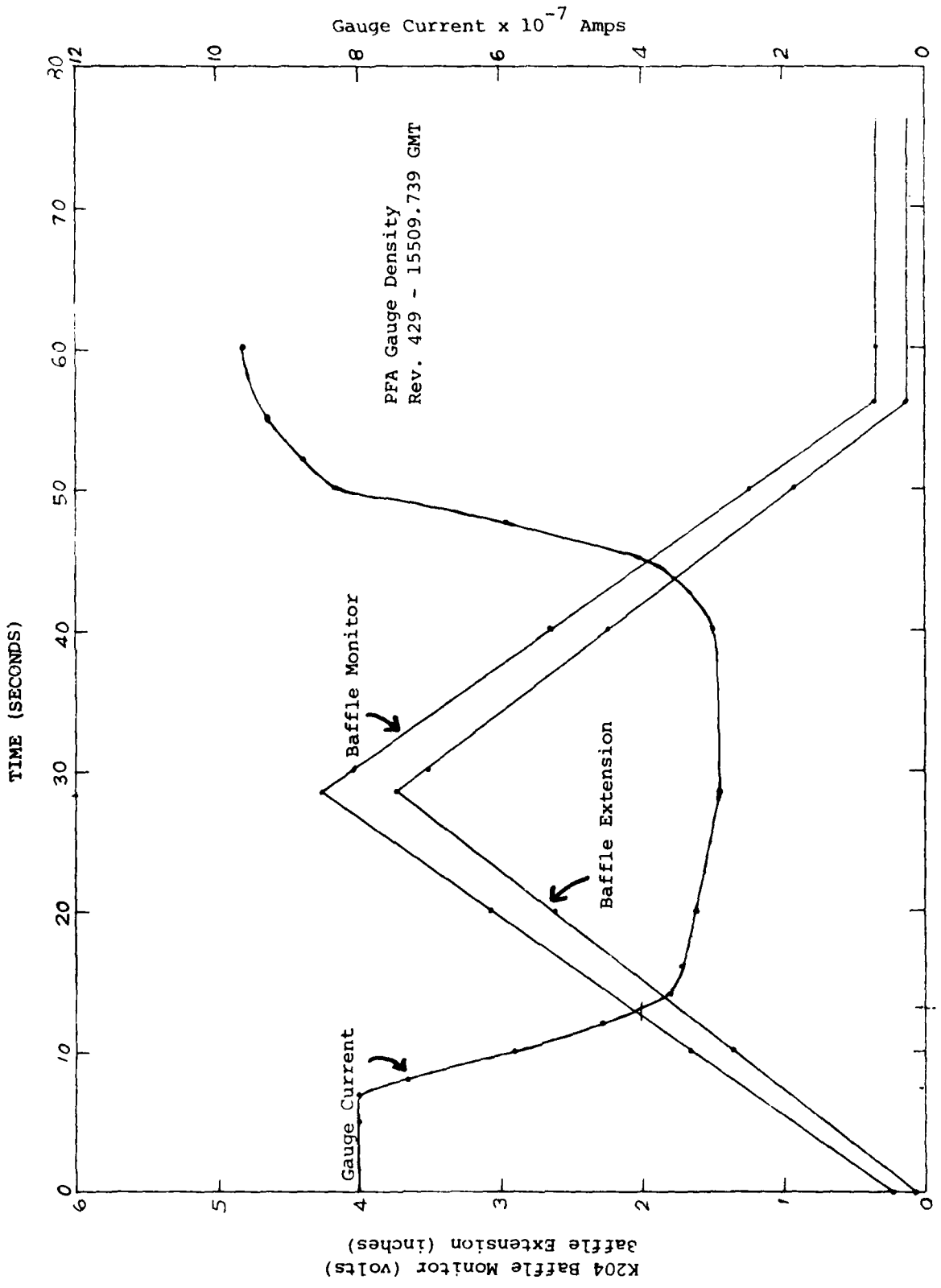


Figure 34 Sample Baffle Deployment

CRL-737 CCG RANGE REV 2159 07/27/78

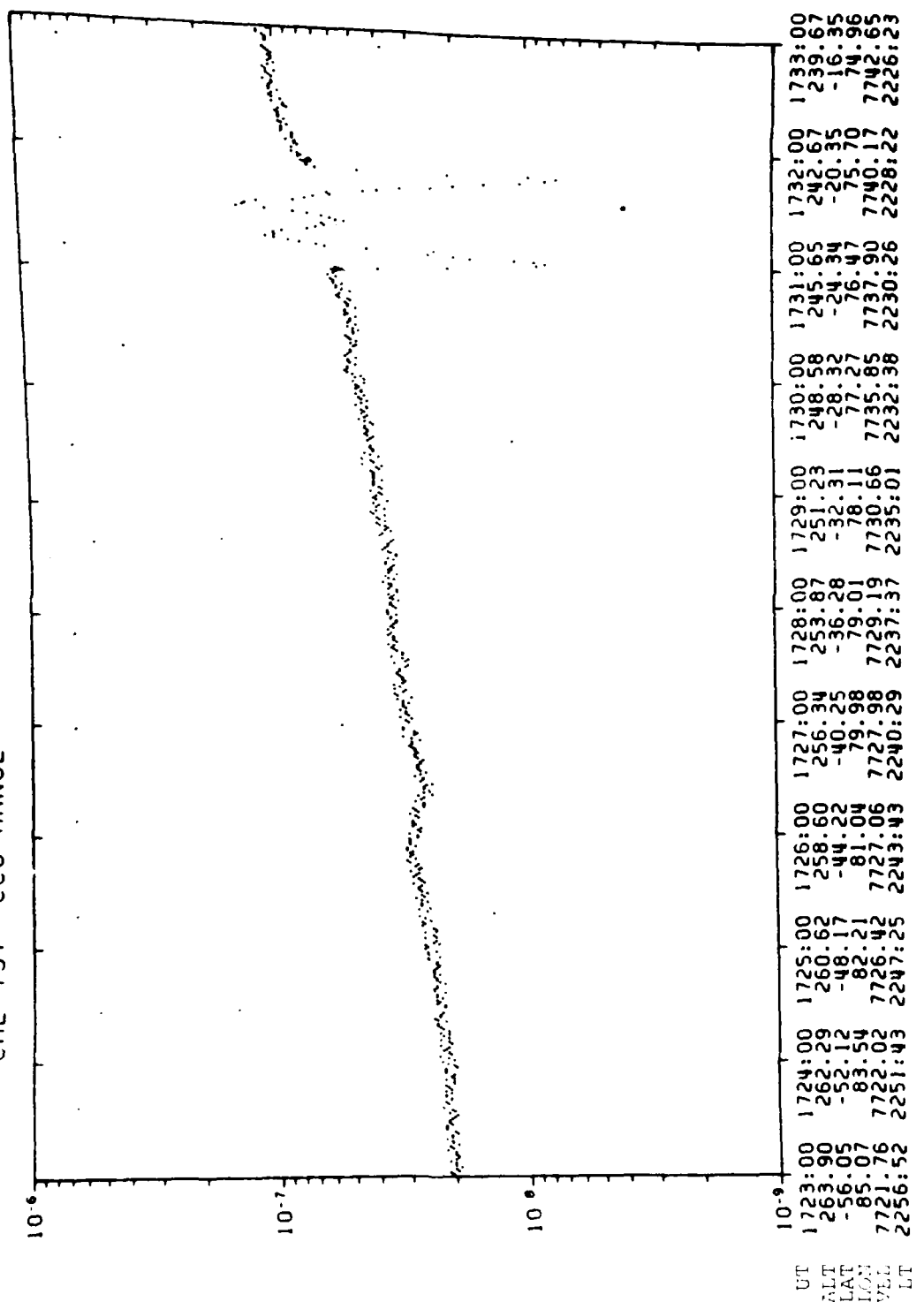
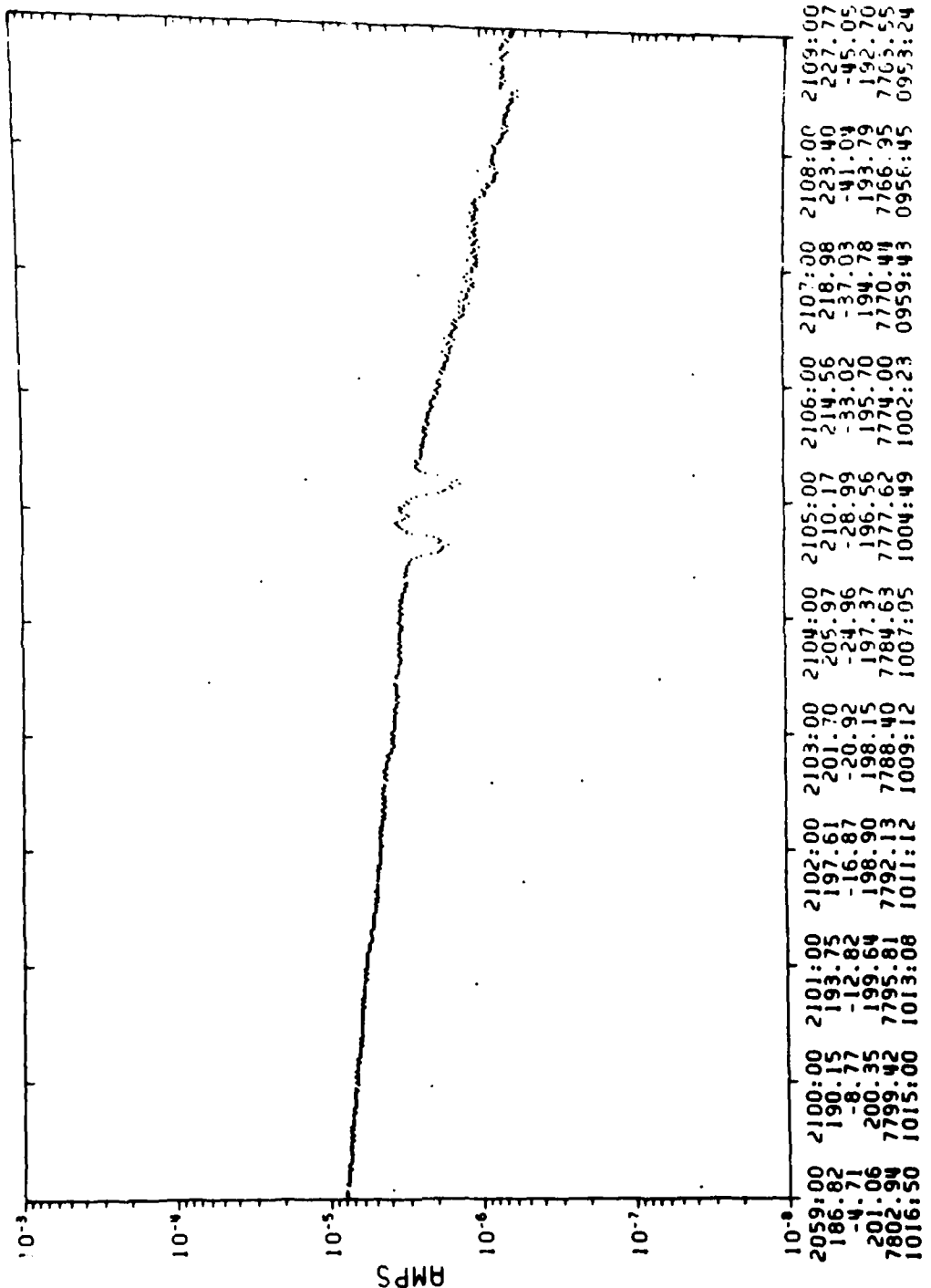


Figure 35 Late Orbit Baffle Deployment

CRL-737 PFA DENSITY REV 2177 07/28/78



UT	ALT	LAT	LON	VEL	LT
2059:00	186.82	-4.71	201.06	7802.94	1016:50
2100:00	190.15	-8.77	200.35	7799.42	1015:00
2101:00	193.75	-12.82	199.64	7795.81	1013:08
2102:00	197.61	-16.87	198.90	7792.13	1011:12
2103:00	201.70	-20.92	198.15	7788.40	1009:12
2104:00	205.97	-24.96	197.37	7784.63	1007:05
2105:00	210.17	-28.99	196.56	7777.62	1004:49
2106:00	214.56	-33.02	195.70	7774.00	1002:23
2107:00	218.98	-37.03	194.78	7770.44	0959:43
2108:00	223.40	-41.04	193.79	7766.35	0956:45
2109:00	227.77	-45.05	192.70	7763.55	0953:24

Figure 36 Late Orbit Baffle Deployment

in the USAF OV15 satellite. In this instance it is stated that the satellite at 325 KM altitude was spinning with a period of ~ 6.5 seconds and the current modulation from 1.6×10^{-7} Amps to 1.5×10^{-8} Amps (3.25 seconds) tracked the pressure change. This gauge did not include perforations in the cathode, however, it contained a baffle structure within the tubulation which neither the PFA nor CCG gauges possess. That the conductance of the OV-15 instrument should be substantially higher than that of the PFA and CCG gauges remains uncertain. More likely, however, the modulation recorded in the OV15 experiment is erroneous since the modulation should have been substantially greater than 10 to 1.

d) General Observations Derived From Complete Orbit Plot

An examination of Figures 37 and 38 which illustrate reduced data over a complete orbit serves well to make some general observations. The remarks apply to plots received for orbits 244, 329, 390, 429 and 445. The transmitted data indicates that later orbits appear similar to those listed, and hence the comments apply over the lifetime of the experiment.

- 1) There is agreement between the two instruments within a factor of 2.5 over a large portion of the orbit (extending from perigee to ~ 255 KM) if we compare the PFA high gain output with the CCG high gain output and correspondingly similar agreement between the PFA low gain output with the CCG low gain output.
- 2) The best agreement appears in the region of ~ 240 KM to 200 KM during which time the satellite is approaching in the direction of perigee. During these passes the CCG instrument is saturated in its high gain channel and the CCG low gain channel output agrees well with both the high and low gain outputs of the PFA.
- 3) The above correlation is not noted for the corresponding altitude range when the satellite travels from perigee to apogee. In general what is observed here is that the CCG instrument tends to read higher values than the PFA.
- 4) For a given gauge, the CCG or PFA, we note differences in the output of the high gain and low gain channels in the overlapping current regions. This is worse for the CCG instrument than the PFA as discussed elsewhere in the report. This feature is evident in Figure 37 if we note the behavior of the density profiles on the high and low gain channel. This effect appears to be related to an electronic oscillation discussed in some detail under the section relating to electronic performance. The oscillation affects the low current operation at the time the Cabot gauges are acquiring data or in the baffle mode of operation. Our belief is that the high sensitivity outputs are more correct than the low sensitivity outputs in the region of the anomaly. The problem does not appear in the auto calibrate mode.

S3-4 C.C.G.
 REV. NO.: 429-0
 DATE: 04/12/78

IN SUN FROM 14400. TO 14747.
 IN SHADE FROM 14747. TO 16937.
 IN SUN FROM 16937. TO 20062.
 IN SHADE FROM 20062. TO 23400.

MODEL DENSITY: X
 M205 DENSITY: O
 M206 DENSITY: A
 MF=4
 F10.7=180.0

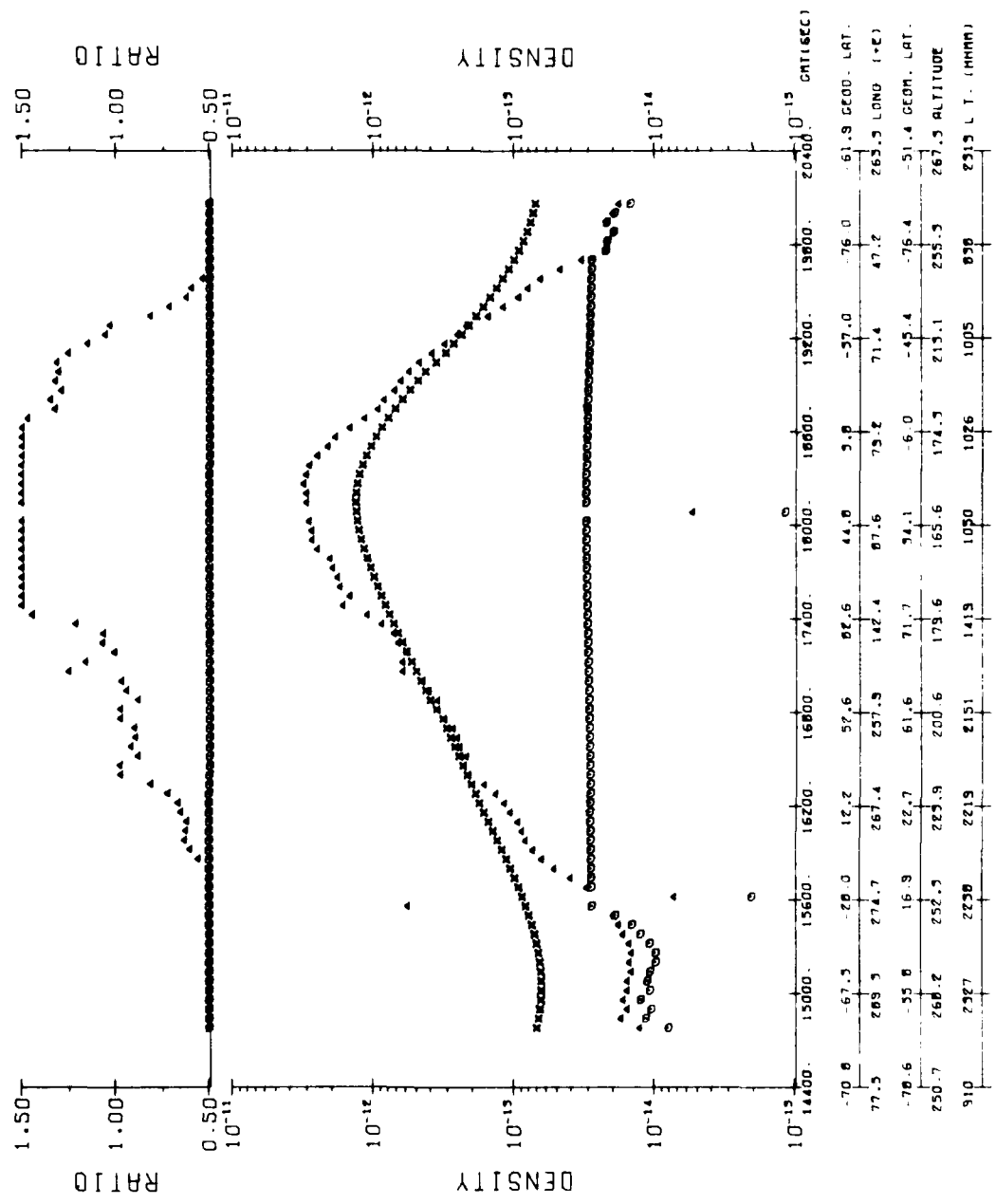


Figure 1. Complete orbit 429 000

S3-4 P.F.R.
 REV. NO.=429-0
 DATE= 04/12/78

IN SUN FROM 14400. TO 14747.
 IN SHADE FROM 14747. TO 18857.
 IN SUN FROM 18857. TO 20082.
 IN SHADE FROM 20082. TO 20400.

MODEL DENSITY= X
 SZ11 DENSITY= O
 SZ01 DENSITY= A
 NP=4
 P10.7=180.0

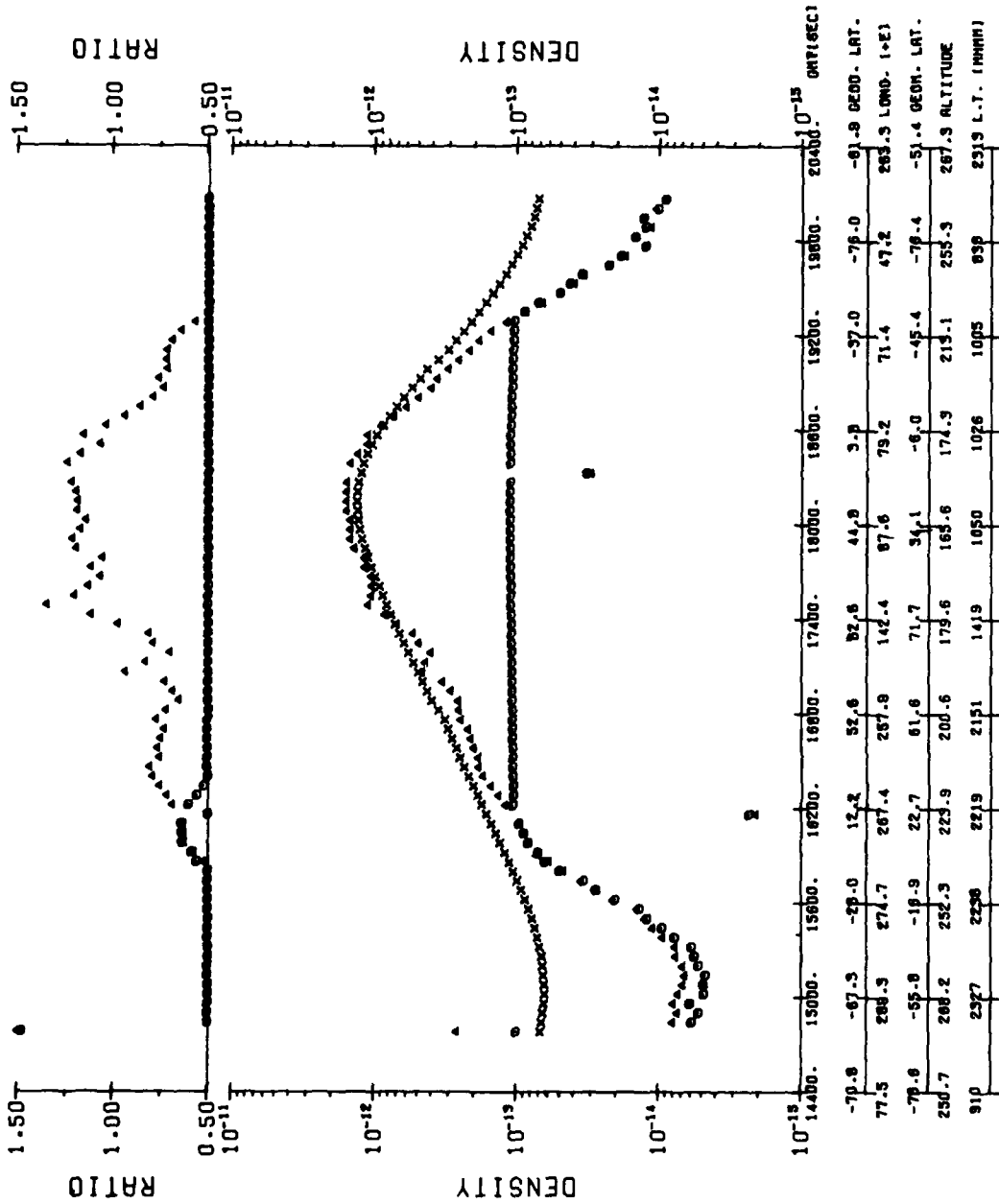


Figure 38 Complete Orbit 429 PFA

- 5) A comparison of both instruments with the model atmosphere indicates that the PFA provides better agreement particularly over the lower altitudes corresponding to the sunlit portions of the orbit.
- 6) The CCG instrument is observed to read the higher currents at all altitudes. Although the sunlit portions of the orbit generally appear to be in somewhat better agreement with the model atmosphere, it is not believed any rational argument can be made to support a solar influence. Hinteregger has reported photoelectric currents of 4×10^{-9} Amps/cm². While the potential for some effect could exist at much higher altitudes particularly in the perforated CCG instrument, this would appear to be precluded in view of the current range (10^{-5} - 10^{-4} Amps) which is recorded in the perigee region.
- 7) The major disagreement between the data and the model atmosphere in the apogee region for both instruments appears inexplicable unless a) one assumes that the gauge orientation has radically changed from the perigee orientation (i.e., satellite reorientation maneuvers), or b) major problems exist with both gauges in terms of their vacuum conductance properties. We have mentioned elsewhere that similar type gauges have been used in satellite programs and seemingly possess the necessary response.
- 8) It has been noted that an overall scale factor shift in one of the instruments whereby the perigee outputs are matched for both instruments leads to a better overall agreement between the two gauges. While this appears tempting we have not been able to account for such a shift. The gauge high voltage variation over many orbits does not warrant such a shift on the basis of the voltage dependent sensitivity changes in the Cabot gauge. We have speculated that perhaps the original pressure calibration performed at the Cabot Corporation indicated differences which may not have been put into the actual data reduction. Although there are some variations as noted in Table 1 in the two instruments we understand that the actual calibration data for each instrument was used in the reduction to the computer plot shown in Figure 37. Speculating further, one is tempted to suggest the possibility that perhaps one of the gauges had undergone some long term deleterious effect to produce the observed differences between the CCG and PFA instruments.
- 9) The intergauge differences, more than likely, are related to the conductance differences in the perforated and the non-perforated cathodes. The evidence pointing in this direction comes from two sources. Firstly, as has been mentioned we note distinct differences in the CCG and PFA gauge comparisons coming from lower pressures (high altitudes) to higher pressures (low altitudes). Secondly, the very significant differences which are described elsewhere concerning the baffle deployment in the PFA instrument compared to the CCG instrument suggest strongly that a lag occurs in the non-perforated gauge. This

is evidenced by the significantly steeper drop to lower current values in the CCG.

Although the decreased conductance argument seems reasonable for the PFA the problem is not completely resolved. That is, while there are differences in the PFA-CCG baffle modulated current profiles the time constant differences amount only to a few seconds at most. The evidence for this is the fact that the recovery to the ambient level is not delayed appreciably even for the PFA (non-perforated). In view of this it is not clear how time constant differences could account for the substantial differences which exist with the model atmosphere in the higher altitude portion of the orbit. The disagreement between model and data argues for a substantially longer time constant or in other words a much poorer conductance than demonstrated in the baffle case.

VII. PERFORMANCE OF ELECTRONIC CIRCUITRY

The operation of the electronic circuitry was found to be quite stable during the entire mission except for two anomalous behavioral effects: 1) a lack of consistence between the range and density outputs for both the CCG and the PFA instruments when operating in the measurement mode with gauge current levels which correspond to the overlap regions of the range and density channels, and 2) a departure from conformance to a logarithmic transfer function for the PFA output when operating in the calibration mode at the low current region.

The anode voltages applied to the two gauges maintained a steady value of $1800 \pm 30V$ as indicated by the monitor outputs. The baffle extend/retract circuitry operated properly throughout the flight and the auto calibration circuitry for each instrument appeared to properly insert a controlled sequence of input currents to the input of its associated electrometer amplifier at the desired rate of about once every 50 seconds.

Under normal circumstances the overlap region provided for the range and density outputs would have been used as a confirmation of the validity of the calibration of the two channels. During pre-delivery measurements at Epsilon Laboratories both at room temperature and over the range of temperatures of $-20^{\circ}C$ and $+70^{\circ}C$ provided by an environmental chamber this appeared to be the case. The tests taken during this period revealed no inconsistencies between the density and the range output signals. Furthermore, the auto-cal input indicated that the system gave stable precise outputs in response to an extended range of input currents.

When the system was operated in its satellite environment, however, significant disagreement was observed between the range channel and the density channel output signals at the lower portion of the overlap region. On the other hand, at the upper portion of the overlap region reasonable agreement was observed. Furthermore, whenever the electronic amplifier had switched to the automatic calibrate mode, excellent agreement was

observed over the entire range of calibration currents. Both the PFA and CCG outputs were similarly affected. One additional effect was noted in the case of the PFA only, that being a departure of the electrometer amplifier output from precise conformance to the required logarithmic transfer function at the low end of the input current range.

The anomalous behavior between the range and density outputs may possibly be caused by a low level oscillation condition in the 8048 integrated circuitry manufactured by Intersil. This unit simultaneously serves both as the electrometer input amplifier and also as the logarithmic converter for the gauge output current. Figure 39, illustrated below, shows the internal circuit details of the 8048 unit. Transistor Q1 forms the feedback element and the output of A1 adjusts itself such that the current through Q1 is just sufficient to balance out the input current which in the case of the CCG and PFA instruments would be the current output of the density gauge.

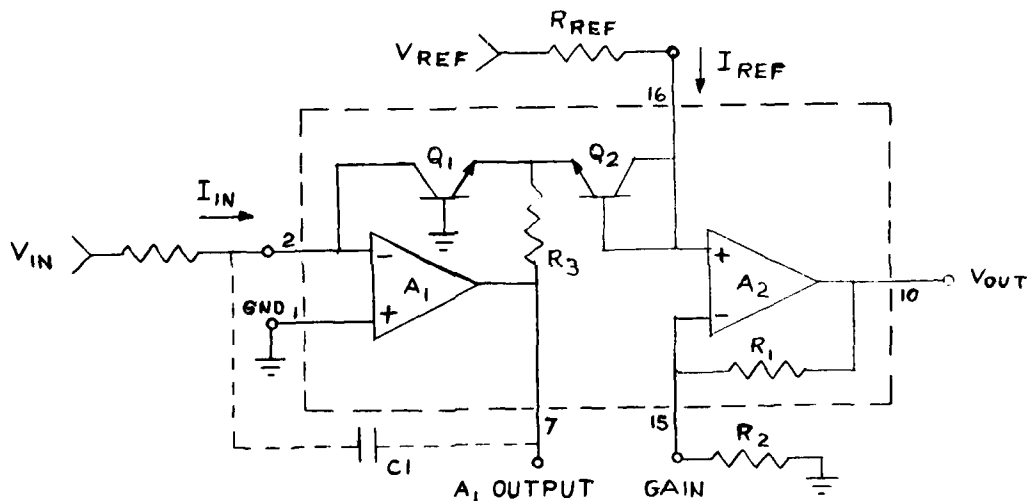


Fig. 39

Q1 is a planar bipolar transistor which is fabricated such as to closely follow the theoretical relation

$$I = I_s \left(e^{\frac{q(V_{be} - V_g)}{KT}} - 1 \right)$$

where I is collector current of Q1 and \$V_{be}\$ is the corresponding base to emitter voltage. From the above equation it is apparent that the emitter

voltage, V_{be} , of Q1 will be proportional to the logarithm of the collector current. Transistor Q1 has a temperature dependent offset voltage and the slope of the logarithmic transfer function is also dependent on temperature. However, the temperature dependence on offset is eliminated using a second identical transistor Q2 to cancel the offset of Q1. The slope variations are compensated for using a second feedback amplifier A2 in which a temperature sensitive feedback resistor R1 is used to compensate for slope changes with temperature. Resistor R3 is incorporated to avoid phase instabilities in A1 under conditions of high input currents. This is required because the dynamic input impedance of Q1 varies inversely with collector current. R3 serves to pad out the excessively high feedback which would have resulted under the condition of high input currents. This condition could have led to amplifier oscillation if resistor R3 had not been incorporated into the circuit.

In order to avoid phase instabilities in the operation of amplifier A1 Intersil suggests that a small capacitor C1 be inserted between the input and output of A1 to provide an additional margin of phase compensation. This capacitance unfortunately introduces an increase in amplifier response time at low input currents because of the inverse relationship of Q1 feedback impedance with input current. At low ambient pressures for which the resulting gauge output current would be low the use of the suggested value of C1 could have resulted in excessively large values of response time. Consequently, the actual value of capacitor C1 which was to have been used was to be determined after the overall effects resulting from capacitances in the amplifier input circuit could be determined when the entire instrument finally came together. The input capacitance results from the cathode capacitance of the gauge, the capacitance of the cable connecting the gauge to the 8048 amplifier and the capacitance of the two protective diode connected field effect transistors which are used to protect the electrometer from possible arc discharges in the gauge. It now appears that the installation of C1 was overlooked in the final stages of assembly and that the logarithmic electrometer amplifiers were very likely delivered with C1 missing.

A representative of Intersil has confirmed that the presence of appreciable values of capacitance at the input of A1 could result in oscillation in the 8048 unit. Furthermore, the possibility of oscillation would be even more likely at low temperatures. Because the actual operating temperature in orbit was below 0°C it is speculated that an oscillation condition existed for both logarithmic amplifiers whenever the gauge output current was less than about 10^{-7} amperes. It is further conjectured that during the calibration mode in which the gauge capacitance, the cable capacitance and the protective diode capacitances are disconnected from the input of the log amplifier by means of the calibration relay, the amplifier would once again be stable and oscillation free. An examination of recorded data obtained during the auto calibration mode appears to confirm that calibration operation was stable over the entire 6 months lifetime of the satellite.

With respect to the effect of any oscillations in the Intersil 8048 log amplifier, the major effect of minor oscillations is such that it will appear to read too low because of an offset error introduced by the nonlinear averaging in Q1. A further error is introduced by one of the two feedback amplifiers which process the output of the log amplifier. The range output and density output are processed by two feedback amplifiers which are identical in every respect except for the insertion of an offset of about 3V into the density amplifier in order to bias it such that it will properly amplify only the upper three decade range of input currents. The "non offset" range channel covers the lower three decade range of input current. Both feedback amplifiers have clamp diodes in the feedback circuit in order to restrict negative excursions. Normally the clamp diodes would never be in a forward biased mode because the signal outputs of the 8048 log amplifiers are normally positive for any input current which is greater than 10^{-9} amperes. However, if the log amplifier is oscillating and processing input currents within the overlap region of the range and density outputs, the a-c signal resulting from the oscillation could cause the clamp diode in the density amplifier to truncate that portion of the oscillation which would have gone below a value of -0.5V d-c. With the negative excursion removed and with the positive excursions still present the average output of the amplifier will be in error by an amount proportional to that portion of the negative going waveform which is clamped out. The net result is that the density amplifier will read high. Because of the low pass filter at the output of the range amplifier no indication of oscillation will be observed by the telemetry data. On the other hand, the range amplifier being biased about 3V more positive will not experience the clamping action unless the oscillation is far more vigorous than is believed to be the case. The average output will correspond to the average input and as in the case of density amplifier, the output filter will eliminate any hint of oscillation.

To summarize the above discussion the electronic design is such that, if an oscillation condition developed in the log amplifier, an error would develop such that the instrument reading would be too low. The amount of error would increase with oscillation amplitude. Furthermore, additional errors introduced by a clamp diode in the density amplifier would cause the density reading to appear to be too high for input currents corresponding to the lower portion of the overlap region of the range and density channels.

The departure of the PFA log amplifier from conformance to a logarithmic transfer characteristic can be explained only be conjecture. The most likely explanation might be the formation of a current leakage path in the input circuit. This could be the result of damage to either one of the diode connected protective FET transistors or to the input section of the 8048 log element itself. The amount of error appears to be small and consistent, therefore it is readily eliminated using the auto-calibration data.

IX. RECOMMENDATIONS

In view of the flight results several improvements for future experiments are suggested. With respect to the internal automatic calibration it is desirable that a second step current be introduced at the top end of the low sensitivity channel. Such a current plateau will facilitate the identity of the starting point of the ramp portion and establish an overall improved time base to check that the calibration has indeed been maintained.

The baffle mode of operation would be significantly improved if a "hold" mode were introduced into the deployment particularly for a few early orbits. Specifically by maintaining the baffle at an extended period for a duration of some tens of seconds one could examine the current profile to observe whether any time constant effect exists for each of the gauges. This would also readily establish whether the efficacy of the perforated CGG gauge is seen in comparison to the PFA. The hold mode would be useful to perform at both high and low altitudes during which times the gauge gas dynamics may differ.

Some additional testing of the gauges themselves prior to launch is indicated. This could include a complete pressure calibration through the entire electronics system. In the present program this was not accomplished due to scheduling difficulties with the available high vacuum facility.

This experiment could also serve to determine whether gauge-electronics capacitive effects exist such as those discussed in the previous section.

The authors wish to acknowledge the assistance and support provided by Mr. Joseph McIsaac of the U. S. Air Force Geophysics Laboratory, Hanscom Air Force Base, MA 01731. We also extend our gratitude to the personnel at the SAMSO program office and to the Lockheed Corporation personnel involved in the satellite integration. Special thanks go to Mr. Theodore Ciesielski, the Epsilon Project Engineer who devoted many hours towards the success of the program.

REFERENCES

1. Satellite Density Gauge Program, T. Ciesielski, AFGL-TR-76-0271, October 1976.
2. Direct Measurements of the Semi Annual Variation During 1968, McIsaac, J. P. and Champion, KSW Space Research XII, 1971
3. Variations of Atmospheric Composition and Density During a Geomagnetic Storm, Philbrick, C. R., McIsaac, J. P. and Faucher, G. A. Space Research XVII, 1977

APPENDIX A

Qualification Testing

In accordance with the requirements specified in the Interface Control Document for the S3-4 payload, qualification testing of the PFA and CCG instruments were performed on the equipments prior to delivery to Lockheed Corporation. The testing performed by Epsilon included vibration tests, thermal vacuum tests and electro magnetic interference tests. The pyro shock tests were conducted at Lockheed Corporation. Mechanical shock testing, acceleration testing and humidity testing were all waived for the PFA and CCG instruments based upon similarity with other experiments in the past. Additionally, a thermal blanket instrument test was conducted to verify the integrity of the S3-4 thermal blanket adjacent to the CCG during the break-off of the entrance tubulation cap. The specific testing conducted included the following:

Quasi-Sinusoidal Vibration

<u>Frequency Range (Hz)</u>	<u>Acceleration - Zero to Peak (g)</u>	<u>Number of Cycles</u>
10 to 25 Nx	6.0	12
2 to 25 Ny	3.0	12
2 to 25 Nz	6.0	12

Random Vibration

<u>Overall (g RMS)</u>	<u>Frequency Range (Hz)</u>	<u>Spectral Density (g²/Hz)</u>
12.0	20 to 100	Increasing at 6 dB/Octave
	100 to 1000	Flat at 0.1 g ² /Hz
	1000 to 2000	Decreasing at 6 dB/Octave

The random vibration was applied to each of three mutually perpendicular axes for a minimum of three minutes. Random vibration tolerance overall level was + 1.5 dB. The vibration tests were conducted at the Air Force Geophysics Laboratory utilizing a "Ling" shaker. The vibration spectrum was controlled by a Time Data computer and the table was instrumented with a Columbia Triaxial accelerometer. Each random vibration was documented with the control spectrum and the accelerometer output spectrum for the two remaining axes. After each test equipment functional performance was checked.

Thermal Vacuum Test: Two complete cycles of thermal vacuum testing were conducted on each system with total time for one cycle approximately 24

hours duration. The thermal vacuum test was conducted as follows:

- a. Perform functional test at ambient temperature and pressure less than 10^{-5} Torr. Turn off instrumentation.
- b. Reduce temperature to -30°F and maintain for one hour. (Note - this step 1st cycle only).
- c. Change temperature to -20°F and maintain for 2 hours. On first cycle turn on instrumentation after one hour at this temperature. On subsequent cycles, (instruments will be on at this time) turn off instrumentation after 1 hour at temperature and then cold start after 1/2 hour of cold soaking. Perform functional test.
- d. Change temperature to 120°F and maintain for 2 hours. After one hour at temperature turn off instrumentation and then hot start after 1/2 hour of hot soaking. Perform functional test.
- e. Change temperature to ambient. Perform functional test.
- f. Subsequent cycles consist of steps c, d and e. Total time for one cycle is approximately 24 hours.

Tests were conducted at the Air Force Geophysics Laboratory utilizing a Tenney chamber capable of hot or cold temperature control and equipped with mechanical and diffusion vacuum pumps. A thermistor served to measure chamber temperature while thermocouple and ionization gauges were used for pressure determination. Temperature was regulated to $\pm 3^{\circ}\text{C}$ and pressure to $\pm 50\%$.

EMI Testing: The EMI testing was conducted at Sanders Associates Corp., Nashua, N.H.. Due to similarity of the PFA and CCG systems only the PFA was subjected to EMI testing. The test consisted of test methods from MIL-STD-826 listed below and other requirements detailed in the Interface Control Document.

<u>Test Method</u>	<u>Test Title</u>
3001	Conducted Interference 30 Hz to 14 KHz
3002	Conducted Interference 14 KHz to 100 MHz
4001	Radiated Interference 14 KHz to 10 GHz
4002	Radiated Interference 20 Hz to 50 KHz, Magnetic Field
5001	Conducted Susceptibility 30 Hz to 150 KHz Modified Limit
5002	Conducted Susceptibility 150 KHz to 400 MHz
5006	Spike Susceptibility (60 V)
6001	Radiated Susceptibility 14 KHz to 10 GHz at 2 V/M
6002	Radiated Susceptibility Induction Field, Spike only

Additional Tests

- a. Ripple Voltage Measurement
- b. Bonding Measurement
- c. Electrical Isolation
- d. Single Event Transients
- e. Low Frequency Ripple Susceptibility

Reports chronologically detailing all pertinent events and measurements of the above tests were submitted to SAMSO, Lockheed Corporation and AFGL.

8-1
FI
D